Gyrokinetic theory of toroidal Alfvén eigenmode saturation via nonlinear wave-wave coupling

Zhiyong Qiu[1,2], Liu Chen[1,2,3] and Fulvio Zonca[1,2]

[1]Institute for Fusion Theory and Simulation, Zhejiang University, Hangzhou, 310027, China.

[2]Center for Nonlinear Plasma Science and ENEA, Frascati, Italy.

[3]Department of Physics and Astronomt, University of California, Irvine, 92697-4575, CA, U.S.A..

Contributing authors: zqiu@zju.edu.cn; liuchen@zju.edu.cn; fulvio.zonca@enea.it;

Abstract

Nonlinear wave-wave coupling constitutes an important route for the turbulence spectrum evolution in both space and laboratory plasmas. For example, in a reactor relevant fusion plasma, a rich spectrum of symmetry breaking shear Alfvén wave (SAW) instabilities are expected to be excited by energetic fusion alpha particles, and self-consistently determine the anomalous alpha particle transport rate by the saturated electromagnetic perturbations. In this work, we will show that the nonlinear gyrokinetic theory is a necessary and powerful tool in qualitatively and quantitatively investigating the nonlinear wave-wave coupling processes. More specifically, one needs to employ the gyrokinetic approach in order to account for the breaking of the "pure Alfvénic state" in the short wavelength kinetic regime, due to the short wavelength structures associated with nonuniformity intrinsic to magnetically confined plasmas.

Using well-known toroidal Alfvén eigenmode (TAE) as a paradigm case, three nonlinear wave-wave coupling channels expected to significantly influence the TAE nonlinear dynamics are investigated to demonstrate the strength and necessity of nonlinear gyrokinetic theory in predicting crucial processes in a future reactor burning plasma. These are: 1.

the nonlinear excitation of meso-scale zonal field structures via modulational instability and TAE scattering into short-wavelength stable domain; 2. the TAE frequency cascading due to nonlinear ion induced scattering and the resulting saturated TAE spectrum; and 3. the cross-scale coupling of TAE with micro-scale ambient drift wave turbulence and its effect on TAE regulation and anomalous electron heating.

Keywords: Gyrokinetic theory, burning plasma, shear Alfvén wave, energetic particles

1 Introduction

Shear Alfvén waves (SAWs) [1] are fundamental electromagnetic fluctuations in magnetised plasmas, and are ubiquitous in space and laboratories. SAWs exist due to the balance of restoring force due to magnetic field line bending and plasma inertia, and are characterized by transverse magnetic perturbations propagating along equilibrium magnetic field lines, with the parallel wavelength comparable to system size, while perpendicular wavelength varying from system size to ion Larmor radius. Due to their incompressible character, SAWs can be driven unstable with a lower threshold, in comparison to that of compressional Alfvén waves or ion acoustic waves. In magnetically confined fusion reactors such as ITER [2] and CFETR [3], with their phase/group velocity comparable to the thermal velocity of super-thermal fusion alpha particles, SAW instabilities could be strongly excited by fusion alpha particles as well as energetic particles (EPs) from auxiliary heating. The enhanced symmetry-breaking SAW fluctuations could lead to transport loss of EPs across magnetic field surfaces; raising an important challenge to the good EP confinement required for sustained burning [4, 5].

In magnetic confined fusion devices, due to the nonuniformities associated with equilibrium magnetic geometry and plasma profile, SAW frequency varies continuously across the magnetic surfaces and form a continuous spectrum [6], on which SAWs suffer continuum damping by mode conversion to small scale structures Landau damped, predominantly, by electrons [7–9]. As a result, SAW instabilities can be excited as various kinds of EP continuum modes (EPMs) as the EP resonant drive overcomes continuum damping [10], or discretised Alfvén eigenmodes (AEs) inside continuum gaps to minimise the continuum damping, among which, the famous toroidal Alfvén eigenmode (TAE) [11–14] is a celebrated example. For a thorough understanding of the SAW instability spectrum in reactors, interested readers may refer to Refs. [4, 5, 15–17] for comprehensive reviews.

The SAW instability induced EP anomalous transport/acceleration/heating rate, depends on the SAW instability amplitude and spectrum via wave-particle resonance conditions [18, 19], which are, determined by the nonlinear saturation mechanisms. The first channel for SAW instability nonlinear saturation is the nonlinear wave-particle interactions, i.e., the acceleration/deceleration of EPs by SAW instability induced EP "equilibrium" distribution function evolution and the consequent self-consistent SAW spectrum evolution, among which there are well-known and broadly used model introduced by Berk et al [20–22] from the analogous to the wave-particle trapping in one-dimensional beam-plasma instability system [23]. More recently, Zonca et al systematically developed the non-adiabatic wave-particle interaction theory, based on nonlinear evolution of phase space zonal structures (PSZS) [5, 24–27], i.e., the phase space structures that are un-damped by collisionless processes. The PSZS approach, by definition of the "renormalised" nonlinear equilibria typically varying in the mesoscale in the existence of microscopic turbulences, self-consistently describes the EP phase space non-adiabatic evolution and nonlinear evolution of turbulence due to varying EP "equilibrium" distribution function, very often in the form of non-adiabatic frequency chirping, and is described by a closed Dyson-Schr$\ddot{o}$dinger model. Both mechanisms are tested and broadly used in interpretation of experimental results as well as large scale numerical simulations, e.g., [28–30]. The other channel for SAW nonlinearity, relatively less explored in large-scale simulations, is the nonlinear wave-wave coupling mechanism, describing SAW instability spectrum evolution due to interaction with other electromagnetic oscillations, and is the focus of the present brief review, using TAE as a paradigm case. These approach developed for TAE and the obtained results, are general, and can be applied to other SAW instabilities based on the knowledge of their linear properties.

The nonlinear wave-wave coupling process, as an important route for SAW instability nonlinear dynamic evolution and saturation, is expected to be even more important in burning plasmas of future reactors; where, different from present-day existing magnetically confined devices, the EP power density can be comparable with that of bulk thermal plasmas, and the EP characteristic orbit size is much smaller than the system size. As a consequence, there is a rich spectrum of SAW instabilities in future reactors [4, 5, 31, 32], with most unstable modes being characterized by $n \gtrsim O(10)$ for maximized wave-particle resonances, with n being the toroidal mode number. That is, multi-n modes with comparable linear growth rates could be excited simultaneously. These SAW instabilities are, thus, expected to interact with each other, leading to complex spectrum evolution that eventually affects the EP transport. It is noteworthy that, the nonlinear wave-particle interaction described by Dyson Schr$\ddot{o}$dinger model and nonlinear wave-wave coupling described by generalized nonlinear Schr$\ddot{o}$dinger equation, are two pillars for the unified theoretical framework for self-consistent SAW nonlinear evolution and EP transport, as summarized in Ref. [24], and is being actively developed by the Center for Nonlinear Plasma Physics (CNPS) collaboration [1].

Due to the typically short scale structures associated with continuum coupling, the nonlinear coupling of SAW instabilities, are dominated by the

[1]For more information and activities of CNPS, one may refer to the CNPS homepage at https://www.afs.enea.it/zonca/CNPS/

perpendicular nonlinear scattering via Reynolds and Maxwell stresses, instead of the polarization nonlinearity [8, 33, 34]. Thus, the kinetic treatment is needed, to capture the essential ingredients of SAW nonlinear wave-wave coupling dominated by small structures naturally occur due to SAW continuum, and some other crucial physics not included in magnetohydrodynamic (MHD) theory, e.g., the wave-particle interaction crucial for ion induced scattering of TAEs [35, 36], and trapped particle effects in the low frequency range that may lead to neoclassical inertial enhancement crucial for zonal field structure (ZFS) generation [37–39]. These crucial physics ingredients are not included in the MHD description, and kinetic treatment is mandatory to both quantitatively and qualitatively study the nonlinear wave-wave coupling processes of SAWs. These features can be fully and conveniently covered by nonlinear gyrokinetic theory [40] derived by systematic removal of fast gyro motions with $\Omega_c \gg \omega_A$, and yield quantitatively, using TAE as a paradigm case, the nonlinear saturation level and corresponding EP transport and/or heating. The general knowledge obtained here, as noted in the context of this review, can be straightforwardly applied to other kinds of SAW instabilities, with the knowledge of their linear properties.

The rest of the paper is organized as follows. In Sec. 2, the general background knowledge of nonlinear wave-wave coupling of SAW instabilities in toroidal are introduced, where SAW instabilities in toroidal plasmas and nonlinear wave-wave coupling are briefly reviewed. The kinetic theories of TAE saturation via nonlinear wave-wave coupling are reviewed in Sec. 3, where three channels for TAE nonlinear dynamic evolution are introduced. Finally, a brief summary is given in Sec. 4.

2 Theoretical framework of nonlinear mode coupling and SAWs in toroidal plasmas

In this section, the fundamental knowledge needed for SAW nonlinear mode coupling is introduced, including the linear SAW dispersion relation, pure Alfvénic state, perpendicular nonlinear coupling, and nonlinear gyrokinetic theoretical framework. For the accessibility of general readers, these materials are introduced in a pedagogical way. Readers interested in more technical details may refer to references given.

2.1 Nonlinear wave-wave coupling

The nonlinear wave-wave coupling corresponds to wave spectrum evolution due to interaction with other collective oscillations, and is an important pillar of nonlinear plasma physics [34]. For SAW instability, there is an important property that, in uniform plasmas and ideal MHD limit, the Reynolds and Maxwell stresses, will exactly cancel each other. Thus, SAWs can grow to large amplitudes without being distorted by nonlinear effects. This is called “pure Alfvénic state”, and will be addressed briefly below. As a result, for the nonlinear mode couplings of SAWs, the pure Alfvénic state shall be broken by, e.g., system nonuniformity and/or kinetic compression, as addressed in Ref. [41].

The momentum equation for the incompressible SAW nonlinear evolution in the low β plasma, keeping up to quadratic terms, can be written as

$$\rho_0(\partial_t + \delta\mathbf{v}\cdot\nabla)\delta\mathbf{v} = \delta\mathbf{J}\times\mathbf{B}_0/c + \delta\mathbf{J}\times\delta\mathbf{B}/c, \tag{1}$$

with ρ being the mass density, $\mathbf{v}$ the fluid velocity, $\mathbf{J}$ the current density, $\mathbf{B}$ the magnetic field, and δ indicating perturbed quantities. Equation (1), together with the Ampere's law

$$\nabla\times\delta\mathbf{B} = 4\pi\delta\mathbf{J}/c \tag{2}$$

and the Faraday's law with ideal MHD condition embedded,

$$\partial_t\delta\mathbf{B} = \nabla\times(\delta\mathbf{v}\times\mathbf{B}_0), \tag{3}$$

yield, in the linear limit,

$$\frac{\delta\mathbf{v}}{V_A} = \pm\frac{\delta\mathbf{B}}{B_0}, \tag{4}$$

which corresponding to the famous Walen relation [42]. In deriving equation (4), the linear SAW dispersion relation, derived from linearised equations (1) and (3), $\omega^2 = k_\parallel^2 V_A^2$ is used, with $V_A \equiv \sqrt{B_0^2/(4\pi\rho_0)}$ being the Alfvén velocity.

Equation (1), in the nonlinear limit, can be re-written as

$$\rho_0\partial_t\delta\mathbf{v}^{(2)} = -\nabla|\delta B|^2/(8\pi) - \mathrm{MX} - \mathrm{RS}, \tag{5}$$

with $\mathrm{MX} \simeq -\delta\mathbf{B}_\perp\cdot\nabla\delta\mathbf{B}_\perp/(4\pi)$ and $\mathrm{RS} \equiv \rho_0\delta\mathbf{v}_\perp\cdot\nabla\delta\mathbf{v}_\perp$ being, respectively, the Maxwell and Reynolds stresses, and the first term on the right hand side corresponding to the parallel ponderomotive force [34], which is typically much smaller than RS and MX due to the typical $k_\parallel \ll k_\perp$ ordering. It can be seen clearly that, in the present model of ideal MHD, uniform plasma limit, RS and MX will cancel each other, so SAW can grow to large amplitude without being distorted by nonlinear processes. Thus, to understand the nonlinear evolution of SAW instabilities as this pure Alfvénic state is broken, higher order nonlinearities that occur on longer time scales should be introduced, or the ideal MHD conditions assumed should be removed. As we shall show in the following applications using TAE as an example, plasma nonuniformity, plasma compressibility may play crucial roles in the corresponding parameter regimes. For a thorough discussion of pure Alfvénic state and SAW/KAW nonlinear dynamics as it is broken by various effects, interested readers may refer to Ref. [41] for more details. As a consequence, to account for these effects, kinetic theory is needed; and for SAWs as well as drift waves (DWs) involved in the analysis with frequencies much lower than ion cyclotron frequency, nonlinear gyrokinetic theory is shown to be extremely powerful in studying the nonlinear wave-wave interaction physics, and is introduced in the Sec. 2.2.

2.2 Nonlinear gyrokinetic theoretical framework

Nonlinear gyrokinetic equation is derived by systematically removal of the fast gyro-motion of particles, noting the conservation of magnetic moment $\mu \equiv mv_\perp^2/(2B)$ in the low frequency regime with $\omega \ll \Omega_c$, and it is a powerful tool in theoretical/numerical studies of low frequency fluctuations of interest in magetically confined plasmas [40, 43]. In gyrokinetic theory, the fluctuating particle response can be separated into adiabatic and non-adiabatic components,

$$\delta f_j = -\left(\frac{q}{T}\right)_j F_{0j}\delta\phi_k + \exp(-\rho\cdot\nabla)\delta H_j, \tag{6}$$

with the non-adiabatic particle response derived from nonlinear gyrokinetic equation [40]

$$\begin{aligned}&\left(\partial_t + v_\parallel \mathbf{b}\cdot\nabla + \mathbf{v}_d\cdot\nabla\right)\delta H_k\\ &= i\frac{q}{m}\left(\omega\partial_E - \omega_*\right)F_0 J_k \delta L_k - \sum_{\mathbf{k}=\mathbf{k}'+\mathbf{k}''}\Lambda^{k'}_{k''} J_{k'}\delta L_{k'}\delta H_{k''}.\end{aligned} \tag{7}$$

Here, $\mathbf{v}_d = \mathbf{b}\times[(v_\perp^2/2)\nabla\ln B_0 + v_\parallel^2\mathbf{b}\cdot\nabla\mathbf{b}]$ is the magnetic drift, $\omega_* \equiv \mathbf{k}\cdot\mathbf{b}\times\nabla\ln F_0/\Omega_c$ is the diamagnetic drift frequency associated with plasma nonuniformities, $\eta = L_n/L_T$ with L_n and L_T being respectively the characteristic scale length of density and temperature nonuniformities, $J_k \equiv J_0(k_\perp\rho)$ is the Bessel function of zero-index accounting for finite Larmor radius effects, $\delta L_k \equiv \delta\phi - v_\parallel\delta A_\parallel/c$, and $\Lambda^{k'}_{k''} \equiv (c/B_0)\mathbf{b}\cdot\mathbf{k}''\times\mathbf{k}'$ for perpendicular scattering with the constraint on wavenumber matching condition given by $\mathbf{k} = \mathbf{k}' + \mathbf{k}''$. In the rest of the paper, $\delta\psi_k = \omega\delta A_{\parallel k}/(ck_\parallel)$ is introduced for conveniently treating the induced field, and ideal MHD condition ($\delta E_\parallel = 0$) can be recovered by straightforwardly taking $\delta\psi_k = \delta\phi_k$. In the present work focusing on the nonlinear evolution of TAE with prescribed amplitude due to nonlinear mode coupling, with dominant role played by thermal plasma contribution to RS and MX [2], in the rest of the manuscript, Maxwellian distribution function is adopted for thermal plasmas, and one has $\partial_E F_M = -(m/T)F_M$.

The governing equations are derived from quasi-neutrality condition

$$\frac{n_0 e^2}{T_i}\left(1 + \frac{T_e}{T_i}\right)\delta\phi_k = \sum_j \langle qJ_k\delta H_k\rangle, \tag{8}$$

[2]We note that, EP can contribute significantly to ZFS generation by TAE as TAEs are exponentially growing due to wave-particle resonance, and lead to the "forced driven" excitation of ZFS by TAE [44, 45]. We, however, will not discuss this case in the present review aiming at giving a fundamental picture of TAE nonlinear dynamics via nonlinear mode coupling.

and, with magnetic compression being negligible in the low-β limit of interest here, the nonlinear gyrokinetic vorticity equation [19, 46]

$$\frac{c^2}{4\pi\omega^2}B\frac{\partial}{\partial l}\frac{k_\perp^2}{B}\frac{\partial}{\partial l}\delta\psi_k+\frac{e^2}{T_i}\left(1-\frac{\omega_*}{\omega}\right)_k\left\langle\left(1-J_k^2\right)F_0\right\rangle\delta\phi_k-\sum_j\left\langle qJ_0\frac{\omega_d}{\omega}\delta H\right\rangle_k$$
$$=-\frac{i}{\omega_k}\sum_{\mathbf{k}=\mathbf{k}'+\mathbf{k}''}\Lambda^{k'}_{k''}\left[\langle e(J_kJ_{k'}-J_{k''})\delta L_{k'}\delta H_{k''}\rangle+\frac{c^2}{4\pi}k''^2_\perp\frac{\partial_l\delta\psi_{k'}\partial_l\delta\psi_{k''}}{\omega_{k'}\omega_{k''}}\right]. \quad (9)$$

Nonlinear gyrokinetic vorticity equation is derived from parallel Ampere's law, quasi-neutrality condition and nonlinear gyrokinetic equation, and it, together with quasi-neutrality condition, equation (8), form a closed set of equations describing the dynamics of low frequency fluctuations in low β plasmas. Note that, for the application in the present review, in equation (9), only effects associated with plasma density nonuniformity are accounted for, while effects associated with temperature gradients are neglected systematically, i.e., $\eta\equiv L_n/L_T=0$. The terms on the left hand side of Eq. (9) are, respectively, the field line bending, inertia and curvature-pressure coupling terms, showing clearly the convenience of vorticity equation in studying SAW related physics, which exist due to balancing of field bending and inertia terms. The terms on the right hand side, on the other hand, are the formally nonlinear generalized gyrokinetic RS and MX, dominated, respectively, by ion and electron contributions.

In this brief review focusing on the TAE physics due to nonlinear wave-wave interactions, TAE with prescribed amplitude are assumed, while EPs contribution is typically small. Thus, we include only the thermal plasma contribution in the above governing equations. The EPs, crucial for the TAE excitation, can also be important in ZFS generation as the TAE is still exponentially growing due to resonant EP drive. This interesting topic of nonlinear ZFS forced driven process through the nonlinear EP response to ZFS will not be the focus of the present review and only be briefly discussed in Sec. 3.1.

Note that, for TAE of interest of the present review, with frequency typically much larger than thermal plasma diamagnetic frequency, the system nonuniformity associated with ω_* are typically weak and are systematically neglected in the majority of present review on TAE nonlinear physics. It is used, however, in Sec. 3.3 on TAE scattering by DWs, where ω_* is crucial for the high-n DW physics, as well as enhancement of nonlinear scattering due to $|\omega_*|\gg|v_i/(qR_0)|$ ordering.

2.3 SAW instabilities in toroidal plasmas

In this section, the SAW dispersion relation in the WKB limit will be derived, which are then used to symbolically demonstrate the formation of SAW continuum structure and the existence of discrete Alfvén eigenmode, using the well-known TAE as an example. The obtained linear particle responses, can be used in the following analysis of TAE nonlinear dynamics via nonlinear wave-wave coupling processes. For the convenience of following analysis on nonlinear wave-wave couplings, the particle responses to SAW, are derived in real space, and the obtained mode equation, will be solved by transforming into ballooning space. Note that for TAE of interest here, $|\omega_*/\omega| \ll 1$ is satisfied for most unstable TAEs with perpendicular wavelength being comparable to EP drift orbit width, the thermal plasma ω_* effects on SAW dispersion relation is expected to be small. In the majority of the paper, the ω_* effects on TAE/KAW dispersion relation is systematically neglected. However, in our derivation of linear thermal plasma response to SAW, ω_* correction is kept, which will be used in Sec. 3.3 where ω_* effects on KAW can be non-negligible due to its relatively high toroidal mode number due to high-n DW scattering.

The linear electron response to SAW, can be derived noting the $|\omega/k_\parallel v_e| \ll 1$ ordering, and one obtains

$$\delta H^{(0)}_{ke} \simeq -\frac{e}{T_e} F_0 \left(1 - \frac{\omega_{*e}}{\omega}\right)_k \delta\psi_k. \tag{10}$$

While for ion response, assuming unity charge for simplicity, and noting the $\omega \gg k_\parallel v_i \gg \omega_d$ ordering, one has, to the leading order,

$$\delta H^{(0)}_{ki} \simeq \frac{e}{T_i} F_0 J_k \left(1 - \frac{\omega_{*i}}{\omega}\right)_k \delta\phi^{(0)}_k. \tag{11}$$

Substituting into quasi-neutrality condition, one obtains,

$$\delta\psi^{(0)}_k = \sigma_{*k}\delta\phi^{(0)}_k, \tag{12}$$

with

$$\sigma_{*k} = \frac{1 + \tau - \tau\Gamma_k(1 - \omega_{*i}/\omega)_k}{(1 - \omega_{*e}/\omega)_k}, \tag{13}$$

$\Gamma_k = I_0(b_k)\exp(-b_k)$ and I_0 being the modified Bessel function. Noting $|k_\perp\rho_i| \ll 1$ and $|\omega_{*i}/\omega| \ll 1$ for most unstable TAEs, one has $\sigma_{*k} \simeq 1$, i.e., ideal MHD condition is satisfied in the lowest order. To the next order, one has

$$\delta H^{(1)}_{ki} \simeq \frac{e}{T_i} F_0 J_k \left(\delta\phi^{(1)}_k + \frac{\omega_{di}}{\omega}\delta\phi^{(0)}_k\right), \tag{14}$$

with $\delta\phi^{(1)}_k$ being derived from quasi-neutrality condition, and contributing to SAW continuum upshift. The particle response can be substituted into linear gyrokinetic vorticity equation, and yields,

$$\tau b_k \epsilon_{Ak}\delta\phi^{(0)}_k = 0, \tag{15}$$

with the SAW operator in the WKB limit given by

$$\epsilon_{Ak} \equiv -\left(\frac{V_A^2}{b}\frac{k_\parallel b k_\parallel}{\omega^2}\right)_k \sigma_{*k} + \frac{1-\Gamma_k}{b_k}\left(1-\frac{\omega_{*i}}{\omega}\right)_k + \left\langle qJ_k\frac{\omega_d}{\omega}\delta H_{ki}^{(1)}\right\rangle \Big/ \left(\frac{n_0 e^2}{T_i}b_k\delta\phi_k^{(0)}\right). \tag{16}$$

The terms of ϵ_{Ak} correspond to field line bending, inertia and curvature coupling terms where ballooning-interchange terms are included, and resonant excitation by EPs can be straightforwardly accounted for by substituting the corresponding EP response into the curvature coupling term. Noting that $b_k \equiv -\partial_\perp^2$ and $k_\parallel$ should be strictly understood as operators, and are not commutative. The SAW instability eigenmode dispersion relation in torus, can be derived by transforming Eq. (15) into ballooning space, and noting the two scale structure of SAW instabilities due to plasma nonuniformity. Here, for simplicity of discussion while relevance to the present work, we focus on modes in the TAE frequency range, and thus, from now on, the curvature coupling term that contributes to SAW continuum upshift and BAE generation, are neglected. The $|\omega_{*i}/\omega|$ correction are also systematically neglected here. The perturbed scalar potential $\delta\phi_k$ can be decomposed as

$$\delta\phi_k = A_k e^{-in\xi - i\omega t + im_0\theta}\sum_j e^{ij\theta}\Phi_j(nq-m_0), \tag{17}$$

with A_k being the radial envelope, m_0 being the reference poloidal mode number, $m = m_0 + j$, and Φ_j being the fine radial scale structure associated with $k_\parallel$. Defining $z = nq - m = k_\parallel q R_0$, η being the Fourier conjugate of z, and

$$\Phi(z) = \int \phi(\eta) e^{-i\eta z} d\eta, \tag{18}$$

the SAW eigenmode equation, equation (15), can be reduced to

$$\left[\frac{\partial^2}{\partial\eta^2} + \Omega_A^2\left(1 + 2\epsilon_0\cos\eta\right) - \frac{\hat{s}^2}{(1+\hat{s}^2\eta^2)^2}\right]\hat{\Phi} = 0, \tag{19}$$

with $\hat{\Phi} \equiv \phi(\eta)/\sqrt{1+\hat{s}^2\eta^2}$, $\hat{s} \equiv rq'/q$ being the magnetic shear, $\Omega_A^2 = \omega^2 q^2 R_0^2/V_A^2$, and $\epsilon_0 = (r/R_0 + \Delta')$ with Δ' being Shafranov shift. Equation (19) has a clear two-scale character, and can be solved by asymptotic matching of two scale structures. For inertial layer contribution with $|\hat{s}\eta| \gg 1$, equation (19) reduces to

$$\left[\frac{\partial^2}{\partial\eta^2} + \Omega_A^2\left(1 + 2\epsilon_0\cos\eta\right)\right]\hat{\Phi}_E = 0, \tag{20}$$

i.e., Mathieu's equation describing mode propagating in periodic systems, which can be solved noting its two scale character,

$$\hat{\Phi}_E = A(\eta)\cos(\eta/2) + B(\eta)\sin(\eta/2), \tag{21}$$

with $A(\eta)$ and $B(\eta)$ being slowly varying with respect to $\cos(\eta/2)$. One then has

$$-B'(\eta) = \left(\Omega^2 - 1/4 + \epsilon_0\Omega^2\right) A \equiv \Gamma_l A, \tag{22}$$

$$A'(\eta) = \left(\Omega^2 - 1/4 - \epsilon_0\Omega^2\right) B \equiv \Gamma_u B, \tag{23}$$

with $\Gamma_l \equiv \Omega^2 - 1/4 + \epsilon_0\Omega^2$ and $\Gamma_u \equiv \Omega^2 - 1/4 - \epsilon_0\Omega^2$determining the lower and upper accummulational points of toroidicity induced SAW continuum gap [11], which then yields,

$$\hat{\Phi}_E(\eta) = a\left(\sqrt{-\Gamma_u}\cos\frac{\eta}{2} \pm \sqrt{\Gamma_l}\sin\frac{\eta}{2}\right)e^{\mp\sqrt{-\Gamma_l\Gamma_u}\eta}. \tag{24}$$

The "±" sign should be chosen in the way such that $e^{\mp\sqrt{-\Gamma_l\Gamma_u}\eta}$ decay as $|\eta| \to \infty$. Noting equation (21) and that η is the Fourier conjugate of $z = k_\parallel qR_0$, the $\cos(\eta/2)/\sin(\eta/2)$-dependence of $\hat{\Phi}_E$ corresponds to mode localization at $|nq-m| = 1/2$, i.e., the two neighbouring poloidal harmonics couple in the middle of two adjacent mode rational surfaces as their respective dispersion relation degenerate, forming the well-known "rabbit-ear" like mode structure. This feature is important for the nonlinear mode coupling processes investigated in Sec. 3, due to the dominant contribution from the radially fast varying inertial layer. The SAW continuum with corrections due to toroidicity, can be obtained from

$$k_\parallel qR_0 = \sqrt{-\Gamma_l\Gamma_u}, \tag{25}$$

which then yields the toroidicity induced SAW continuum gap formation, inside which the discrete TAE can be excited with minimized continuum damping. A sketched continuum is shown in Fig. 1. The corresponding discrete Alfvén eigenmode, i.e., TAE, can then be excited by, e.g., EPs, inside this toroidicity induced continuum gap, with minimized requirement on EP drive due to the minimized continuum damping [12, 13]. The TAE excitation mechanism, however, is beyond the scope of the present review, focusing on the nonlinear evolution of TAE with prescribed amplitude due to nonlinear wave-wave coupling, and will not be addressed here.

3 TAE saturation via nonlinear wave-wave coupling

Nonlinear mode coupling describes the TAE distortion due to interaction with other oscillations, and is expected to play crucial role in TAE nonlinear

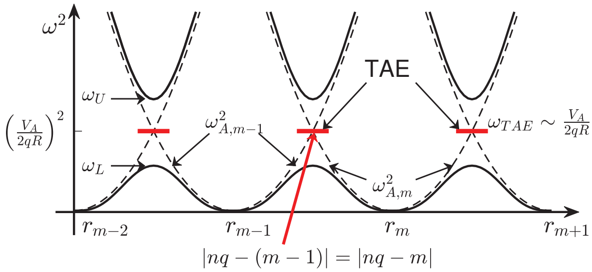

Fig. 1 Toroidicity induced SAW continuum gap. The horizontal axis is radial position with r_m denoting the $q = m/n$ rational surface, and vertical axis corresponds to ω^2. The dashed and solid curves correspond to the SAW continuum in the cylindrical and toroidal limits, respectively; and ω_U and ω_L denote the upper and lower accumulational points of toroidicity induced continuum gap.

saturation in future reactors with system size being much larger than characteristic orbit size of EPs, and, thus, SAW instabilities with a broad spectrum in toroidal mode numbers can be simultaneously excited by EPs. To illustrate the richness of nonlinear mode couplings of TAE and the powerfulness of gyrokinetic theory in the investigation, three examples are presented, i.e., the nonlinear excitation of $n = 0$ zonal field structure (ZFS) by TAE [39], which corresponds to single-n TAE nonlinear envelope regulation via modulational instability; nonlinear spectral evolution of TAE via ion induced scattering [35, 36], which is expected to play crucial role in determining the multiple-n TAE saturated spectrum and thus EP transport; and cross-scale scattering and damping of meso-scale TAE by micro-scale DW [47], as motivated by recent experiments as well as simulations showing improved thermal plasma confinement in the presence of significant amount of EPs [48–50]. All three presented channels are shown to significantly influence the TAE nonlinear dynamics from different aspects, and their relative importance and implications on TAE saturation in burning plasma parameter regimes are discussed. As many notations are involved, in the following subsections on three difference nonlinear channels, the notations of "pump", "sideband" and the corresponding nonlinear coupling coefficients used, are defined only in the corresponding subsection.

3.1 ZFS generation by TAE

Zonal field structures correspond to toroidally and poloidally symmetric perturbations with $n = 0$, and are thus, linearly stable to expansion free energy associated with plasma profile nonuniformities. ZFS can be nonlinearly excited by DW turbulence including drift Alfvén waves (DAWs), and in this process, self-consistently scatter DW/DAW into linearly stable short radial wavelength domain, leading to turbulence regulation and confinement improvement. ZFS excitation was extensively studied in the DWs dynamics [38, 51–53], observed in simulations with TAEs [44, 54], and the theory was originally generalized to the nonlinear physics of TAE [39]. The nonlinear excitation process can be

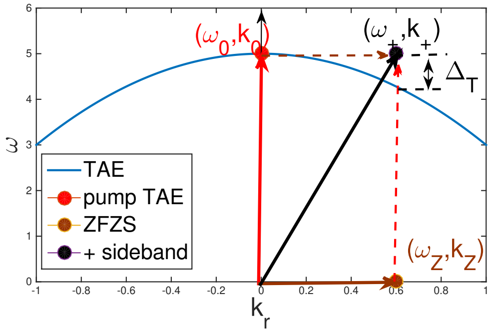

Fig. 2 Frequency and wavenumber matching condition for ZFS generation by TAE. Here, the horizontal axis is the radial envelope wavenumber k_r, and vertical axis is the frequency. The solid curve is the TAE dispersion relation, and Δ_T is the frequency mismatch.

described by the four-wave modulational instability, where upper/lower TAE sidebands due to ZFS modulation are generated, and the nonlinear dispersion relation for ZFS generation can be obtained by the coupled ZFS and TAE sidebands equations. It is noteworthy that, both electrostatic zonal flow (ZF) and electromagnetic zonal magnetic field (zonal current, ZC) should be accounted for on the same footing for the proper understanding of the ZFS generation process [39, 55].

For the clarity of presentation, we focus on the modulational instability of TAE originally investigated in Ref. [39]. The further extensions, including the enhanced nonlinear coupling due to existence of "fine-radial-scale" structure ZFS [56], and effects of resonant EPs in rendering the ZFS generation process into a forced driven process [45], will be only briefly discussed at the end of this section to give the readers a complete picture of the state-of-art achievements. Considering the TAE constitutes the pump wave $\Omega_0(\omega_0, \mathbf{k}_0)$ and its upper and lower sidebands $\Omega_\pm(\omega_\pm, \mathbf{k}_\pm)$ due to the radial modulation of ZFS $\Omega_Z(\omega_Z, \mathbf{k}_Z)$, and assuming $\Omega_\pm = \Omega_Z \pm \Omega_0$ as the wave vector/frequency matching conditions, the perturbations can be decomposed as

$$\begin{aligned}
\delta\phi_0 &= A_0 e^{i(n\phi - m_0\theta - \omega_0 t)} \sum_j e^{-ij\theta} \Phi_0(x-j), \\
\delta\phi_\pm &= A_\pm e^{\pm(n\phi - m_0\theta - \omega_0 t)} e^{i(\int k_Z dr - \omega_Z t)} \sum_j e^{\mp ij\theta} \left\{ \begin{array}{c} \Phi_0(x-j) \\ \Phi_0^*(x-j) \end{array} \right\}, \\
\delta\phi_Z &= A_Z e^{i(\int k_Z dr - \omega_Z t)}.
\end{aligned}$$

The frequency and wavenumber matching conditions are already assumed, as illustrated in Fig. 2. We note that, the expression of $\delta\phi_\pm$ indicates that the parallel mode structure (Φ_0) is not altered by the radial envelope modulation process, which occurs on a longer time scale than the formation of the parallel mode structure.

We start from ZFS generation. The first equation for zonal flow generation can be derived from nonlinear vorticity equation. Noting that ZFS have $k_{\parallel Z} = 0$, one obtains

$$\frac{n_0 e^2}{T_i}\left\langle(1-J_Z^2)\frac{F_0}{n_0}\right\rangle\delta\phi_Z - \sum_{s=e,i}\left\langle\overline{\frac{q}{\omega}J_Z\omega_d\delta H_Z^{(1)}}\right\rangle$$
$$= -\frac{i}{\omega_Z}\sum_{\mathbf{k}'+\mathbf{k}''=\mathbf{k}_Z}\Lambda_{k''}^{k'}\left[\langle e(J_Z J_{k'} - J_{k''})\delta L_{k'}\delta H_{k''}\rangle + \frac{c^2}{4\pi}k_\perp''^2\frac{\partial_l\delta\psi_{k'}\partial_l\delta\psi_{k''}}{\omega_{k'}\omega_{k''}}\right].$$

Substituting ion responses of Ω_0 and $\Omega_\pm$ into RS, noting $k_\perp\rho_i \lesssim O(1)$, and averaging over fast varying radial scale, one obtains

$$i\omega_Z\hat{\chi}_{iZ}\delta\phi_Z = -\frac{c}{B_0}k_{\theta 0}k_Z\left(1-\frac{\omega_A^2}{4\omega_0^2}\right)(A_0A_- - A_{0^*}A_+). \tag{26}$$

Here, $\hat{\chi}_{iZ} \equiv \chi_{iZ}/(k_Z^2\rho_i^2)$, with $\chi_{iZ} \simeq 1.6k_Z^2\rho_i^2q^2/\sqrt{\epsilon}$ corresponds to the neoclassical inertial enhancement [37], $\omega_A = V_A/(qR_0)$ and $1-\omega_A^2/(4\omega_0^2) \sim O(\epsilon)$ corresponds to the RS and MX non-cancellation due to toroidicity, and finite coupling comes from radial envelope modulation ($\propto k_Z^2\rho_i^2$) by ZFS.

The zonal magnetic field equation can be derived from electron parallel force balance equation in stead of the quasi-neutrality condition,

$$\delta E_\parallel + \mathbf{b}\cdot\delta\mathbf{u}_\perp\times\delta\mathbf{B}_\perp = 0. \tag{27}$$

Noting that $\delta E_\parallel \equiv -\nabla_\parallel\delta\phi - \partial_t\delta A_\parallel$, $\delta\mathbf{u}_\perp \simeq \nabla_\perp\delta\phi\times\mathbf{b}/B$, $\delta\mathbf{B}_\perp = \nabla\times\delta A_\parallel\mathbf{b}$, and introducing the effective potential due to the induced parallel electric field $\delta\psi_k = (\omega\delta A_\parallel/ck_\parallel)_k$ for TAEs while $\delta\psi_Z = \omega_0\delta A_{\parallel Z}/(ck_{\parallel 0})$ for zonal component, one obtains,

$$\delta\psi_Z = -\frac{i}{\omega_0}\frac{c}{B_0}k_Z k_{\theta 0}(A_0A_- + A_{0^*}A_+). \tag{28}$$

In deriving Eq. (28), we also noted $\omega_\pm = \omega_Z \pm \omega_0$ as well as ideal MHD condition for TAEs.

The TAE sidebands equations can be derived from nonlinear vorticity equation. We will start with the upper sideband, while the derivation of the governing equations for the lower sideband is similar. Neglecting the curvature coupling term due to the $|\omega| \gg \omega_G$ ordering for TAEs, substituting the linear ion responses to Ω_0 and Ω_Z into equation (9), and noting $k_\perp\rho_i \lesssim O(1)$, we have

$$k_{\perp +}^2\left[-k_{\parallel 0}^2\delta\psi_+ + \frac{\omega_+^2}{V_A^2}\delta\phi_+\right] = -i\frac{c}{B_0}k_Z k_{\theta 0}\left(k_Z^2 - k_{\perp 0}^2\right)\frac{\omega_0}{V_A^2}\delta\phi_0(\delta\phi_Z - \delta\psi_Z) \tag{29}$$

The other equation for Ω_+ can be derived from the electron parallel force balance equation, equation (27), noting that $k_{0\parallel} = k_{+\parallel}$ and $\delta\phi_0 \simeq \delta\psi_0$ for the pump TAE, and we obtain:

$$\delta\phi_+ - \delta\psi_+ = i\frac{c}{B_0}k_Z k_{0\theta}\frac{1}{\omega_0}\delta\phi_0\left(\delta\psi_Z - \delta\phi_Z\right). \tag{30}$$

Substituting equation (30) into (29), one then have

$$b_+\epsilon_{A+}\delta\phi_+ = 2\frac{i}{\omega_0}\frac{c}{B_0}k_{0\theta}k_Z b_0\delta\phi_0\left(\delta\phi_Z - \delta\psi_Z\right), \tag{31}$$

with ϵ_{A+} being the Ω_+ dispersion relation in the WKB limit. The Ω_- equation can be derived similarly. Multiplying both sides of equation (31) by Φ_0 and averaging over the radial scale, one has

$$b_\pm\hat{\epsilon}_{A\pm}A_\pm = 2\frac{i}{\omega_0}\frac{c}{B_0}k_{0\theta}k_Z b_0\begin{pmatrix}A_0\\A_0^*\end{pmatrix}\left(\delta\phi_Z - \delta\psi_Z\right), \tag{32}$$

with

$$\hat{\epsilon}_{A\pm} = \left(\omega_A^4\Lambda_T(\omega)D(\omega,k_Z)/\epsilon_0\right)_{\omega=\omega_\pm}, \tag{33}$$

$$D(\omega,k_Z) = \Lambda_T(\omega) - \delta\hat{W}(\omega,k_Z), \tag{34}$$

$\Lambda_T \equiv \sqrt{-\Gamma_l\Gamma_u}$ as given by equation (25), and $\delta\hat{W}(\omega,k_Z)$ being the normalized potential energy.

The modulational dispersion relation for ZFS generation by TAE can then be derived from equations (26), (28), and (32), and one obtains

$$2\left(\frac{c}{B_0}k_Z k_{0\theta}|A_0|\right)^2\frac{b_0}{b_Z}\left[\frac{1-\omega_A^2/(4\omega_0^2)}{\hat{\chi}_{iZ}(\omega_Z/\omega_0)}\left(\frac{1}{\hat{\epsilon}_{A+}} - \frac{1}{\hat{\epsilon}_{A-}}\right) + \left(\frac{1}{\hat{\epsilon}_{A+}} + \frac{1}{\hat{\epsilon}_{A-}}\right)\right]$$
$$= -1, \tag{35}$$

which can be solved by expanding $D(\omega_\pm,k_Z)$ as

$$D(\omega_\pm,k_Z) = \pm\frac{\partial D}{\partial\omega_0}\left(i\gamma_Z \mp \Delta_T\right), \tag{36}$$

with $\gamma_Z = -i\omega_Z$ and $\Delta_T \equiv \omega_T(k_Z) - \omega_0$ being the frequency mismatch as shown in Fig. 2, and one obtains

$$\gamma_Z^2 = \left(\frac{c}{B_0}k_Z k_\theta|A_0|\right)^2\frac{b_0}{b_Z}\frac{\epsilon_0}{\Lambda_T}\frac{4\omega_0/\omega_A^2}{\partial D_0/\partial\omega_0}\left[\frac{\Delta_T}{\omega_0}\frac{\omega_0^2}{\omega_A^2} + \frac{1}{\hat{\chi}_{iZ}}\left(\frac{\omega_0^2}{\omega_A^2} - \frac{1}{4}\right)\right] - \Delta_T^2, \tag{37}$$

with the first term in the square brackets ($\propto \Delta_T/\omega_0$) corresponding to the contribution from ZC, while the other term from ZF contribution. It is readily seen that, ZF contribution can be of higher order due to the neoclassical shielding ($1/\hat{\chi}_{iZ} \ll 1$) and RS-MX near cancellation by $\omega_0^2/\omega_A^2 - 1/4 \sim O(\epsilon)$. Thus, for $\Delta_T/\omega_0 > 0$, ZC excitation can be preferred due to its much lower threshold condition on pump TAE amplitude A_0. On the other hand, for $\Delta_T/\omega_0 < 0$, ZF excitation is still possible, however, on quite stringent conditions, i.e., $\omega_0^2/\omega_A^2 > 1/4$ which corresponds to the pump TAE lies within the upper half of the toroidicity induced continuum gap [57], and the pump TAE amplitude being large enough to overcome the threshold due to frequency mismatch. It thus suggests that, ZFS is dominated by ZC due to the trapped-ion enhanced polarizability, thus, a kinetic treatment is necessary. On the other hand, if MHD model without trapped particle effects is adopted, the obtained ZFS excitation condition and corresponding ZFS level will be qualitatively in-correct. It was also noteworthy that, the argument that "ZC excitation is preferred" is also related to the TAE of interest here, for which RS and MX nearly cancel each other. This argument cannot be straightforwardly generalized to other SAW instabilities, e.g., BAE with $|k_\parallel V_A/\omega| \ll 1$ will predominantly excite ZF [58, 59]; while for reversed shear Alfvén eigenmode (RSAE) with frequency between TAE and BAE frequency range, depending on the specific $|nq_{min} - m|$ value, both ZF and/or ZC excitation can be preferred [60].

For ZC excitation with $\Delta_T/\omega_0 > 0$ and typical parameters of most unstable TAE with $k_\perp \rho_E \sim O(1)$, the threshold condition can be estimated as

$$\left|\frac{\delta B_{r0}}{B_0}\right|^2 \sim O(10^{-8} \sim 10^{-7}), \tag{38}$$

which is consistent with the observed magnetic perturbations in present day tokamak experiments [61], suggesting the ZFS excitation can be important for TAE saturation. As the drive by pump TAE is significantly higher than the threshold, the ZFS growth rate is proportional to pump TAE amplitude, typical of spontaneous excitation processes by modulational instability, demonstrating the region spontaneous excitation is dominant, in comparison to, e.g., the forced driven process with the ZFS growth rate determined by the instaneous TAE growth rate, as discussed below [45, 62].

In the present analysis, only thermal plasma contribution to inertial layer is considered; consistent with EP contribution being negligible in the perpendicular scattering process due to the $k_\perp \rho_E \gg 1$ ordering. The EP response, however, can enter the ideal region through curvature ballooning term, as addressed in Ref. [45], where it was shown that, as the pump TAE is exponentially growing due to resonant EP contribution, nonlinear EP response to ZFS will contribute to the curvature-pressure term in the vorticity equation, with its amplitude dominant over the RS and MX in the uniform plasma limit. This EP enhanced coupling occur in the exponentially growing stage of the pump

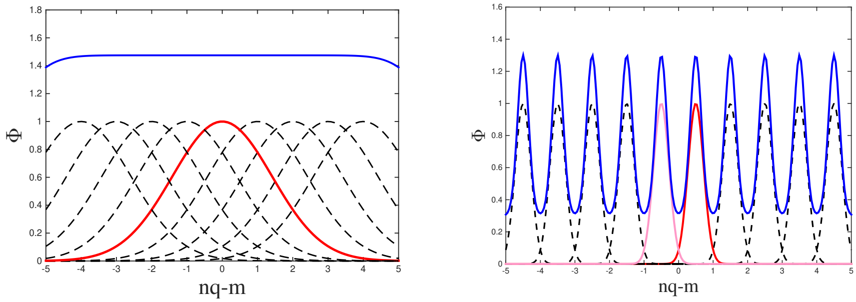

Fig. 3 Cartoon for ZFS excitation by strongly ballooning DWs (left panel) v.s. weakly ballooning SAW instabilities (right panel). Here, the dashed curves correspond to the parallel mode structure $\Phi_0(nq-m)$ for DWs (left panel) and SAW instabilities (right panel), respectively; while the solid blue curves in both panels correspond to $\sum_m |\Phi_0|^2$. Thus, for DWs with $\sum_m |\Phi_0|$ being almost independent of r [52], radial envelope modulation leads to meso-scale ZF excitation; while for SAW instabilities, fine-scale structure ZFS is excited.

TAE, with ZF excitation dominating over ZC contribution. Here, the ZF excitation process corresponds to a "forced driven" process, with the ZF growth rate being twice of the instaneous TAE growth rate, as frequently observed in numerical simulations [44, 50, 62].

Another important finding on ZFS excitation by SAW instabilities is, due to the weak/moderate ballooning features of SAW instabilities, the width of the parallel mode structure is comparable or smaller than the corresponding distance between mode rational surfaces. As a result, different from the well-known "meso"-scale ZF excitation in the typically moderately/strongly ballooning DWs, the ZFS excited by TAE has, in addition to the meso-scale radial envelope corrugation, an additional fine-scale radial structure [58, 59], as shown in Fig. 3. This fine-scale radial structure may significantly enhance the ZFS generation and its impact on regulating SAW instabilities via the perpendicular scattering. For a comprehensive review of gyrokinetic ZFS by TAE, interested readers may refer to Ref. [56] where different physics, e.g., forced driven v.s. spontaneous excitation, meso-scale corrugation v.s. fine-scale structure, are clarified.

3.2 TAE saturation due to ion induced scattering

Nonlinear ion induced scattering is another potentially important channel for SAW instability nonlinear saturation, corresponds to SAW instabilities parametric decay into another SAW and a heavily ion Landau damped ion quasi-mode [34], and was originally introduced in Ref. [35] for TAE saturation. This process is of particular interest in that, TAEs lie between two neighbouring mode rational surfaces, and are characterized by finite parallel wavenumber $|k_\parallel| \simeq 1/(2qR_0)$, as discussed in Sec. 2.3. Thus, as two counter-propagating TAEs couple, a low frequency mode with finite parallel wavenumber, i.e., an ion quasi-mode can be generated, that can be heavily ion Landau damped, leading to significant consequence on TAE nonlinear dynamics. Compared to

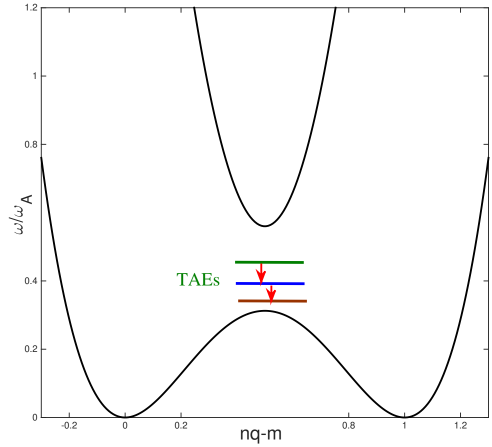

Fig. 4 Cartoon of TAE parametric decay in the low-β limit.

ZFS generation investigated in the previous section as a self-interaction process of a single-n TAE, ion induced scattering process is expected to be of particular importance in reactor scale machines with system size being much larger than the characteristic orbit width of fusion alpha particles, and TAEs with multiple toroidal mode numbers and comparable linear growth rates could coexist [5, 31, 32]. Thus, the ion induced scattering process, can determine the saturated spectrum of TAEs and the consequent alpha particle transport rate. The Landau damping of the nonlinearly generated ion quasi-mode will indirectly transfer the fusion alpha particle power to heat deuterium and tritium ions, providing a potential effective alpha-channeling mechanism [63–68].

The TAE saturation via ion induced scattering was originally investigated in Ref. [35] using drift kinetic theory, which was generalized to fusion relevant short wavelength regime with $k_\perp^2\rho_i^2 \gg \omega/\Omega_{ci}$ in Ref. [36]. Correspondingly, the dominant nonlinear scattering mechanism is qualitatively replaced by the perpendicular scattering [33], and the saturation level is consequently reduced by one order of magnitude. However, the working flow of Ref. 36 is similar to that of Ref. [35]. In a single scattering process, a pump TAE decays into a counter-propagating sideband TAE and an ion quasi-mode, and the parametric decay process can spontaneous occur as the sideband TAE frequency is lower than that of the pump wave, as shown in Fig. 4. This process may lead to TAE saturation as the sideband TAE is continuum damped due to the enhanced coupling to lower accumulational point of SAW continuum. As there are many TAEs co-existing, each TAE may simultaneously interact with many TAEs; in some processes it may act as the pump wave, while in some other processes it acts as the decay wave. To study this spectral cascading process, the interaction of a representative “test” TAE with a “background” TAE is studied; and the equation for the test TAE nonlinear evolution due to interacting with the background TAE is derived by considering the feedback of the background TAE and the ion quasi-mode to the test TAE. In the limit with multiple background TAEs simultaneously interacting with the test TAE, a summation over the background TAEs is taken, and one then obtains, from the imaginary part of the nonlinear equation, the equation describing TAE spectral evolution. It can be used to derive the nonlinear saturation spectrum and the electromagnetic fluctuation induced alpha particle transport rate.

Thus, with the linear instability spectrum determined by the equilibrium profiles, the nonlinear process gives the nonlinear saturation spectrum, which eventually determines the electromagnetic fluctuation induced alpha particle transport, as sketched in Fig. 5.

3.2.1 Parametric decay instability

Starting from the nonlinear interaction of the test TAE $\Omega_0(\omega_0, \mathbf{k}_0)$ with the counter-propagating background TAE $\Omega_1(\omega_1, \mathbf{k}_1)$, during which the ion sound mode (ISM) $\Omega_s(\omega_s, \mathbf{k}_s)$ fluctuation is generated, our analysis involves the coupled equations of ISM generation and background TAE evolution. Considering the $k_{\parallel s} v_e \gg \omega_s, \omega_{ds}$ ordering, and assuming electrostatic ISM, the linear thermal plasma response to ISM can be derived as

$$\delta H_{si}^{(1)} = \frac{e}{T_i} F_{M0} \frac{\omega_s}{\omega_s - k_{\parallel s} v_\parallel} J_s \delta\phi_s, \tag{39}$$

$$\delta H_{se}^{(1)} = 0. \tag{40}$$

Adopting the linear electron response to TAEs derived in Eq. (10), the nonlinear gyrokinetic equation for electron response to ISW becomes

$$\begin{aligned} v_\parallel \partial_l \delta H_{se}^{(2)} &= - \sum_{\mathbf{k}'+\mathbf{k}''=\mathbf{k}} \Lambda_{k''}^{k'} \delta L_{k'} \delta H_{k''e} \\ &\simeq -\Lambda_{k_0}^{k_1^*} \frac{e}{T_e} F_0 v_\parallel \left(\frac{k_{\parallel 1^*}}{\omega_{1^*}} - \frac{k_{\parallel 0}}{\omega_0} \right) \delta\phi_0 \delta\psi_{1^*}, \end{aligned} \tag{41}$$

with $\Lambda_{k_0}^{k_1^*} \equiv (c/B_0)\hat{\mathbf{b}} \cdot \mathbf{k_0} \times \mathbf{k_{1^*}}$. Noting that $\omega_{1^*} \simeq -\omega_0$, $k_{\parallel 1^*} \simeq k_{\parallel 0}$ and consequently that $k_{\parallel s} \simeq 2k_{\parallel 0}$, one has

$$\delta H_{se}^{(2)} \simeq -i \frac{\Lambda_{k_0}^{k_1^*}}{\omega_0} \frac{e}{T_e} F_0 \delta\phi_0 \delta\psi_{1^*}. \tag{42}$$

Nonlinear ion response to Ω_s can be derived noting the $\omega_s \sim k_{\parallel s} v_\parallel \gg \omega_{ds}$ ordering, and one has

$$\delta H_{si}^{(2)} \simeq -i \frac{\Lambda_{k_0}^{k_1^*}}{\omega_0} \frac{e}{T_i} F_0 \frac{k_{\parallel s} v_\parallel}{\omega_s - k_{\parallel s} v_\parallel} J_0 J_1 \delta\phi_0 \delta\phi_{1^*}. \tag{43}$$

It is noteworthy that, $\omega_s \sim k_{\|s} v_\|$ is crucial for the resonant wave-particle interactions that determines the scattering process. Substituting Eqs. (41) and (43) into quasi-neutrality condition, one obtains the nonlinear equation for Ω_s generation:

$$\epsilon_s \delta\phi_s = i\frac{\Lambda_{k_0}^{k_1^*}}{\omega_0}\beta_1 \delta\phi_0 \delta\phi_{1^*}, \tag{44}$$

with $\epsilon_s \equiv 1 + \tau + \tau\Gamma_s \xi_s Z(\xi_s)$ being the ISW linear dispersion relation, $\xi_s \equiv \omega_s/(k_{\|s} v_{it})$, $Z(\xi_s)$ being the well-known plasma dispersion function defined as

$$Z(\xi_s) \equiv \frac{1}{\sqrt{\pi}} \int_{-\infty}^{\infty} \frac{e^{-y^2}}{(y - \xi_s)} dy,$$

the nonlinear coupling coefficient $\beta_1 = 1 + \tau F_1(1 + \xi_s Z(\xi_s))$ and $F_1 \equiv \langle J_0 J_1 J_s F_{0M}/n_0 \rangle$.

The nonlinear particle response to the test TAE, can be derived as

$$\delta H_{0e}^{(2)} = -\frac{(\Lambda_{k_0}^{k_1^*})^2}{\omega_0^2}\frac{e}{T_e} F_0 |\delta\phi_1|^2 \delta\phi_0, \tag{45}$$

$$\delta H_{0i}^{(2)} = i\frac{\Lambda_{k_0}^{k_1^*}}{\omega_0}\frac{e}{T_i} F_0 \frac{k_{\|s} v_\|}{\omega_s - k_{\|s} v_\|}\left[J_1 J_s \delta\phi_s \delta\phi_1 - i\frac{\Lambda_{k_0}^{k_1^*}}{\omega_0} J_1^2 J_0 |\delta\phi_1|^2 \delta\phi_0 \right]. \tag{46}$$

In deriving $\delta H_{0e}^{(2)}$ and $\delta H_{0i}^{(2)}$, the nonlinear particle responses to Ω_s are also included due to the fact that it may be heavily ion Landau damped. One then obtains,

$$\delta\psi_0 = \left(1 + \sigma_0^{(2)}\right) \delta\phi_0 + D_0 \delta\phi_1 \delta\phi_s, \tag{47}$$

with $\sigma_0^{(2)} \equiv (\Lambda_{k_0}^{k_1^*})^2 \left[-1 + \tau F_2(1 + \xi_s Z(\xi_s)\right] |\delta\phi_1|^2/\omega_0^2$, $D_0 = i\tau\Lambda_{k_0}^{k_1^*} F_1[1 + \xi_s Z(\xi_s)]/\omega_0$, and $F_2 = \langle J_0^2 J_1^2 F_0/n_0 \rangle$.

The other equation of Ω_0 can be derived from nonlinear vorticity equation as

$$b_0 \left[\frac{1 - \Gamma_0 + \alpha_0^{(2)}/\omega_0^2}{b_0} \delta\phi_0 - \frac{k_{\|0}^2 V_A^2}{\omega_0^2} \delta\psi_0 \right] = D_2 \delta\phi_1 \delta\phi_s, \tag{48}$$

with

$$\begin{aligned} \alpha_0^{(2)} &= (\Lambda_{k_0}^{k_1^*})^2 (F_2 - F_1)(1 + \xi_s Z(\xi_s))|\delta\phi_1|^2, \\ D_2 &= -i\Lambda_{k_0}^{k_1^*}[F_1(1 + \xi_s Z(\xi_s)) - \Gamma_s \xi_s Z(\xi_s) - \Gamma_1]/\omega_0. \end{aligned}$$

From equations (47), (48) and (44), one obtains the following nonlinear eigenmode equation of the test TAE Ω_0 due to interacting with the background TAE Ω_s

$$b_0\left(\epsilon_{A0}+\epsilon_0^{(2)}\right)\delta\phi_0=-\frac{(\Lambda_{k_0}^{k_1^*})^2\beta_1\beta_2}{\tau\epsilon_s}|\delta\phi_1|^2\delta\phi_0, \tag{49}$$

with $\beta_2\equiv\beta_1-\epsilon_s$. Multiplying both sides of Eq. (49) with Φ_0^*, and averaging over the radial length of $1/(n_sq')\ll\delta\ll 1/(n_0q')$, one then obtains

$$\left(\hat{\epsilon}_{A0}-\Delta_0|A_1|^2-\chi_0\epsilon_s|A_1|^2\right)A_0=-(\hat{C}_0/\epsilon_s)|A_1|^2A_0, \tag{50}$$

with $\hat{\epsilon}_{A0}$ being the Ω_0 linear eigenmode dispersion relation obtained from $\hat{\epsilon}_{A0}\equiv\int|\Phi_0|^2\epsilon_{A0}dr$, Δ_0, χ_0 and $\hat{C}_0$ corresponding, respectively, to nonlinear frequency shift, ion Compton scattering and shielded-ion scattering. Their specific expressions can be found in Ref. [36]. Equation (50) can be understood as the parametric dispersion relation for $\delta\phi_1$ decaying into $\delta\phi_0$ and $\delta\phi_s$ and the condition for the nonlinear process to occur can be determined for different parameter regimes that crucially enter through the properties of $\delta\phi_s$.

For typical tokamak parameters with $\tau\sim O(1)$, Ω_s is heavily Landau damped with $|\epsilon_{s,I}|$ comparable to $|\epsilon_{s,R}|$. One then has, from the imaginary part of equation (50),

$$\gamma+\gamma_0=\frac{|A_1|^2}{\partial_{\omega_0}\epsilon_{0,R}}\left(\frac{\hat{C}}{|\epsilon_s|^2}+\chi_0\right)\epsilon_{s,I}. \tag{51}$$

with $\hat{C}$ and χ_0 corresponding, respectively, to the shielded-ion and nonlinear ion Compton scatterings. Since both $\hat{C}$ and χ_0 are positive definite, and that $\epsilon_{s,I}=\sqrt{\pi}\tau\Gamma_s\xi_s\exp(-\xi_s^2)$ with $\xi_s\equiv(\omega_0-\omega_1)/|k_{\parallel s}v_{it}|$, one then has, $\gamma>0$ corresponds to $\omega_1>\omega_0$, i.e., the parametric decay spontaneously occur as the pump TAE frequency is higher than the sideband TAE. Thus, the above discussed parametric decay process will lead to power transfer from higher frequency part of the spectrum to the lower frequency part [34, 35], as shown in Fig. 5. The sideband TAE, with lower frequency, can be saturated due to enhanced continuum damping to the lower part of the SAW continuum.

3.2.2 Spectral evolution

The spontaneous power transfer from $\delta\phi_1$ to $\delta\phi_0$ investigated above can lead to TAE scattering to the lower frequency fluctuation spectrum. In burning plasma of reactor scale tokamak with multiple TAEs coexist, characterized by comparable frequencies and growth rates, each TAE can interact with the turbulence "bath" of background TAEs, and this process can be described by an equation for spectral evolution derived from Eq. (50). Denoting the generic test TAE with subscript k and background TAE with subscript k_1,

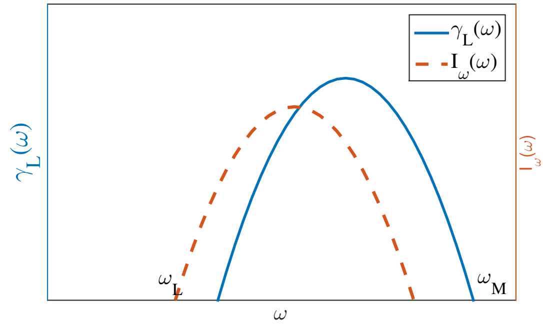

Fig. 5 Cartoon of TAE spectral cascading due to ion induced scattering. The horizontal axis is the mode frequency, solid curve is the linear growth rate while the dashed curve is the saturated spectrum due to ion induced scattering.

and summarizing over all background TAEs, one obtains

$$\hat{\epsilon}_{Ak}A_k = \sum_{k_1}\left(\Delta_0 + \chi_0\epsilon_s - \frac{\hat{C}_0}{\epsilon_s}\right)|A_{k_1}|^2 A_k, \tag{52}$$

Multiplying Eq. (52) with A_k^*, and taking the imaginary part, we then obtain the equation describing TAE nonlinear evolution due to interaction with turbulence bath of TAEs:

$$(\partial_t - 2\gamma_{L,k})\, I_k = \frac{2}{\partial_{\omega_k}\hat{\epsilon}_{Ak,R}}\sum_{k_1}\frac{1}{k_{\perp 1}^2}\left(\frac{\hat{C}}{|\epsilon_s|^2} + \chi_0\right)\epsilon_{s,i}I_{k_1}I_k, \tag{53}$$

which can be rewritten as

$$(\partial_t - 2\gamma_L(\omega))\, I_\omega = \frac{2}{\partial_\omega\epsilon_{\omega,R}}\int_{\omega_L}^{\omega_M} d\omega' V(\omega,\omega')I_{\omega'}I_\omega, \tag{54}$$

with $I_\omega = \sum_k I_k\delta(\omega-\omega_k)$ being the continuum version of I_k, ω_M being the highest frequency for TAE to be linearly unstable, and ω_L being the lowest frequency of TAE spectrum, which is, in fact, linearly stable, and nonlinearly excited in the downward cascading process, as shown by Fig. 5. The integration kernel $V(\omega,\omega')$ is given by

$$V(\omega,\omega') \equiv \frac{1}{k_{\perp\omega'}^2}\left(\frac{\hat{C}}{|\epsilon_s|^2} + \chi_0\right)\epsilon_{s,i}. \tag{55}$$

The saturated TAE spectrum can thus be derived from the fixed point solution of Eq. (54) by taking $\partial_t I_\omega = 0$. The obtained integral equation, can be reduced to a differential equation noting that $I_{\omega'}$ varies in ω' much slower than $V(\omega,\omega')$, with the former varying on the scale of $|\omega_M - \omega_L| \simeq \epsilon_0\omega_A$, while the latter on the scale of $|v_{it}/(qR_0)|$ determined by $\epsilon_{s,i}$. Thus, noting $I_{\omega'} = I_\omega - \omega_s\partial_\omega I_\omega$, $V(\omega,\omega')$ varying in ω much faster than I_ω, and $|\omega_M - \omega_L| \sim \epsilon_0\omega_A \gg \omega_s$ for the ion induced scattering process to be important as shown in Fig. 4, one has

$$\begin{aligned}\gamma_L(\omega) &= -\frac{1}{\partial_\omega\epsilon_{\omega,R}}\int_{\omega-\omega_M}^{\omega-\omega_L} d\omega_s V(\omega_s)\left(I_\omega - \omega_s\partial_\omega I_\omega\right)\\ &= -\frac{1}{\partial_\omega\epsilon_{\omega,R}}\left[U_0 I_\omega - U_1\partial_\omega I_\omega\right].\end{aligned} \tag{56}$$

with

$$U_0 \equiv \int_{\omega-\omega_M}^{\omega-\omega_L} d\omega_s V(\omega_s) \simeq \int_{-\infty}^{\infty} d\omega_s V(\omega_s) \to 0, \tag{57}$$

$$\begin{aligned}U_1 &\equiv \int_{\omega-\omega_M}^{\omega-\omega_L} d\omega_s\omega_s V(\omega_s) \simeq \int_{-\infty}^{\infty} d\omega_s\omega_s V(\omega_s)\\ &\simeq \frac{\pi^{3/2}}{2k_\perp^2}\left(\frac{\hat{C}}{|\epsilon_s|^2} + \chi_0\right)k_{\parallel s}^2 v_{it}^2.\end{aligned} \tag{58}$$

In deriving equations (57) and (58), it is noted that $V(\omega_s) \propto \epsilon_{s,i}$ is odd function of ω_s. Equation (56) is the desired differential equation for the saturated spectrum, and gives

$$I_\omega = \frac{2k_{\parallel s}v_{it}\omega_M\gamma_L(\omega_M)}{U_1} - \frac{1}{U_1}\int_\omega^{\omega_M}\gamma_L\partial_\omega\epsilon_{\omega,R}d\omega, \tag{59}$$

which, after integrating over the fluctuation population zone, yields the overall TAE intensity

$$I_{Sat} \equiv \int_{\omega_L}^{\omega_M} I_\omega d\omega \simeq \frac{\overline{\gamma_L}}{U_1}\omega_T^3\epsilon_{eff}^2, \tag{60}$$

with $\epsilon_{eff} \equiv 1 - \omega_M/\omega_L \sim O(\epsilon)$. Noting that $|\delta B_r|^2 \simeq |k_\theta\delta A_\parallel|^2 = |ck_\theta k_\parallel/(\omega k_r)|^2 I_{Sat}$, one then obtains the saturation level of the magnetic fluctuations

$$|\delta B_r|^2 \simeq \frac{c^2\epsilon^2\epsilon_{eff}^2}{2\pi^{3/2}}\frac{\omega_T\overline{\gamma_L}k_r^2}{(\hat{C}/|\epsilon_s|^2 + \chi_0)\Omega_{ci}^2\rho_{it}^2}, \tag{61}$$

which then yields, for typical parameters in burning plasma regime, the scaling law for the magnetic perturbations,

$$\left|\frac{\delta B_r}{B_0}\right|^2 \sim \frac{m_i}{8\tau\pi^{3/2}e^2\mu_0}\frac{\overline{\gamma_L}}{\omega_T}\frac{T_E^2}{T_i^2}q^2 N_0^{-1}\epsilon^6 R_0^{-2}$$

$$\sim 1.2 \times 10^{15} A_m q^2 N_0^{-1} \epsilon^6 R_0^{-2} \frac{T_E^2}{T_i^2} \frac{\overline{\gamma_L}}{\omega_T}. \tag{62}$$

For typical parameters of reactors, e.g., ITER [2] or CFETR [3], the expected magnetic fluctuation level is $|\delta B_r/B_0|^2 \sim O(10^{-8} \sim 10^{-7})$. It is noteworthy that, the obtained TAE magnetic perturbation, depends sensitively on the local inverse aspect ratio ϵ, which is, however, not surprise, as TAE exist due to toroidicity ($\propto \epsilon$) induced SAW continuum gap, and the saturation process determined by ion-induced scattering, is the TAE downward spectrum cascading (by $\sim \epsilon\omega_A$) that lead to enhanced coupling to SAW continuum.

3.2.3 EP transport

The TAE induced fusion alpha particle transport, can be obtained from nonlinear gyrokinetic transport theory [9, 18], with the expected magnetic fluctuation level given by equation (62). Here, taking circulating EP as an example, whose transport is mainly caused by resonance overlapping induced EP orbit stochasticity [69]. The quasilinear transport equation for EP equilibrium distribution function evolution is [18, 70]

$$\partial_t F_{0E} = -\overline{\sum_{\mathbf{k}=\mathbf{k}'+\mathbf{k}''} \Lambda^{k'}_{k''} J_{k'} \delta L_{k'} \delta H_{k''}}, \tag{63}$$

with $\mathbf{k} = k_Z \hat{\mathbf{r}} = \mathbf{k}' + \mathbf{k}''$ denoting the bounce averaged phase space zonal structure modulation [26] in the radial direction, and the perturbed linear EP distribution function, for well circulating EPs, can be given by [45, 71]

$$\delta H_{kE} = -\frac{e}{m} Q_k F_{0E} J_k \delta L_k \sum_{l,p} \frac{J_l(\hat{\lambda}_k) J_p(\hat{\lambda}_k) e^{-i(l-p)(\theta-\theta_{0r})}}{\omega_k - k_\parallel v_\parallel + l\omega_{tr}}, \tag{64}$$

with $\hat{\lambda}_k = k_\perp \hat{v}_d/\omega_{tr}$ denoting finite drift orbit width effects, and $\theta_{0r} \equiv \tan^{-1}(k_r/k_\theta)$. Substituting equation (64) into equation (63) and integrating over velocity space, one then obtains,

$$\partial_t N_{0E} \simeq -\partial_r D_{Res} \partial_r N_{0E}, \tag{65}$$

with the resonant circulating EP radial diffusion rate given as

$$D_{Res} \equiv \left\langle 2\pi \sum_l |\delta V_{Er,l}|^2 J_l^2(\hat{\lambda}_l) \delta(\omega - k_\parallel v_\parallel + l\omega_{tr}) \frac{F_{0E}}{N_{0E}} \right\rangle, \tag{66}$$

and $|\delta V_{Er,l}| \equiv c k_\theta J_k |\delta\phi_k| l\omega_{tr}/(B_0\omega_k)$ being the resonant EP electric-field drift velocity. Substituting the saturated TAE fluctuation given by equation (61) into equation (66), and noting again $|\delta\phi|^2 = \omega^2\delta B_r^2/(c^2 k_\theta^2 k_\parallel^2)$, one obtains,

$$D_{Res} \simeq \frac{1}{4}\frac{V_A}{k_{\parallel 0}}\left|\frac{\delta B_r}{B_0}\right|^2, \tag{67}$$

corresponding to the resonant EP transit time $\omega_{tr,Res}^{-1}$ being the de-correlation time. The scaling law for TAE induced circulating EP diffusion rate can be derived as

$$D_{Res} \sim 1.3 \times 10^{31} A_m^{1/2} \epsilon^6 q^3 N_{0E}^{-3/2} R_0^{-1} \frac{T_E^2}{T_i^2}\frac{\overline{\gamma_L}}{\omega_T}. \tag{68}$$

For typical parameters of a reactor-size tokamak, the TAE induced resonant circulating EP diffusion rate can be estimated as $D_{Res} \sim 1 - 10 m^2/s$ for $\epsilon \sim 1/6 - 1/3$.

3.2.4 Open questions

The present analysis of TAE saturation via nonlinear ion-induced scattering, extended the previous analysis using drift kinetic theory [35], and gave a more quantitatively accurate estimation of the TAE saturation level and, thus, fusion alpha particle transport rate. For a predictive ability of the impact on fusion plasma performance, besides validation of the present analytical results using first-principle-based large scale simulations, there are several factors remain to be explored.

First, the present analysis neglected the nonuniformity of bulk plasma, and focused on the scattering off ion quasi mode. It is shown in the nonlinear parametric decay of kinetic Alfvén wave (KAW) that, bulk plasma nonuniformity may significantly affect the nonlinear process, by enhancing the ion Compton scattering by an order of magnitude as $|\omega_{*i}| \gg |k_{\parallel s} v_{it}|$, and qualitatively breaking the parity of the decay KAW spectrum that may have an implication on finite momentum transport [72]. As the TAE cascading process of interest in the present review has a one-to-one correspondence to the KAW parametric decay in slab geometry, we expect thermal plasma nonuniformity may also have an important consequence on the TAE saturation, and will be further explored [73].

Second, the nonlinearly generated ion quasi-mode in the present analysis, or drift sound wave as bulk plasma nonuniformity is accounted for, are both heavily ion Landau damped, thus, provide a channel for nonlinearly transfer the alpha particle power to fuel deuterium-tritium ions, as originally proposed and investigated in Ref. [63] based on the results from Ref. [35]. Deriving the ion heating power from the present results and evaluating the implications to sustained burning, are of crucial importance for reactors with high temperature plasma and thus low collisonality.

The third point to be explored is, from the derived local transport given by equation (68), to evaluate the alpha particle global transport, and the steady state alpha particle as well as bulk plasma profile of reactors, by considering the feedbacks of alpha particle driven instabilities to bulk plasmas via different channels [48, 49, 74].

3.3 TAE scattering and damping by DW turbulence

The last nonlinear process to be discussed is the scattering by DW turbulence. Microscopic DW turbulence driven by expansion free energy associated with plasma nonuniformities is another significant low frequency fluctuation in magnetically confined plasmas, and is crucial for thermal plasma transport [75]. DWs typically have frequencies being comparable to plasma diamagnetic frequency, and perpendicular wavelength being comparable to thermal ion Larmor radius. With different free energy sources, DWs may be driven as ion temperature gradient mode, trapped electron modes, and dominant different frequency range of the spectrum. Effects of DWs on EP transport were investigated in Refs. [76, 77], and it is found that, the direct EP transport by DWs can be negligible due to the scale separation between EP orbit size and typical DW perpendicular wavelength. On the other hand, EP may influence the DWs stability via many mechanisms, such as thermal ion dilution [78], modification of curvature by increased pressure gradient [79], etc. For the reference of EP stabilization of DW turbulence, interested readers may refer to a recent review by Citrin et al [80].

With the two fundamental fluctuations coexisting, characterized by distinct spatial and temporal scales, and dominating transport of different energy range, it is natural to consider their effects on each other. The nonlinear interactions of DWs and SAW instabilities via the mediation of ZFS have been proposed and investigated numerically, and was proposed to interpret the experimental observation of confinement improvement with large fraction of EPs [48–50, 81]. This indirect channel remains to be investigated with more care due to the high challenge associated with the complex nonlinear behaviours. It was proposed, in our recent work, that the DWs and SAW instabilities, can interact with each other via direct nonlinear mode coupling processes, which can lead to, e.g., suppression of TAE due to the scattering by the finite amplitude electron DW (eDW) [47]. The "inverse" process of eDW stability in the existence of finite amplitude TAE, on the other hand, shows that TAE has negligible effects on the eDW stability [74]. The paradigm proposed using TAE and eDW as example, can be generalized to include other effects such as trapped electron contribution. Here, we will briefly review the TAE scattering by finite amplitude eDW.

The TAE-eDW scattering process, can be understood as the test TAE "linear" stability in the presence of finite amplitude eDW, and can be considered as a two-step process, i.e., in the first process, short wavelength upper and lower kinetic Alfvén wave (KAW) sidebands are generated, with the frequency comparable to TAE while high toroidal mode number determined by eDW; which then couple with eDW and feed back on the stability of the test TAE, as

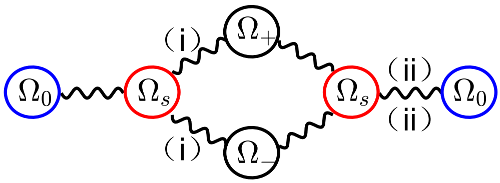

Fig. 6 Cartoon of the two-step nonlinear process of TAE scattering by eDW. The first process corresponds to short scale KAW sidebands generation due to eDW scattering, while the second corresponds to feedback to the test TAE.

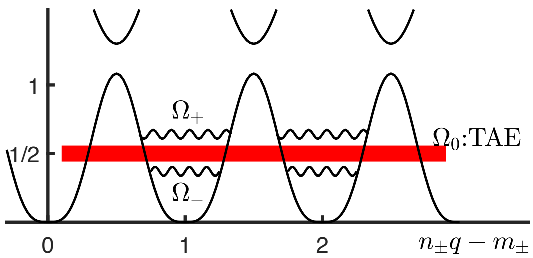

Fig. 7 Cartoon of upper and lower KAWs generation due to TAE-eDW scattering, and coupling to continuum.

shown in Fig. 6. The damping of the mode-converted upper and lower KAWs, as shown in Fig. 7, then lead to the damping of the test TAE.

3.3.1 KAW generation

We start from the upper sideband Ω_+ generation channel due to test TAE Ω_0 and eDW Ω_s coupling, while the analysis for Ω_- is similar. The linear and nonlinear particle responses to Ω_+, can be derived noting the $k_\parallel v_{te} \gg \omega_+ \gg k_\parallel v_{ti}$ ordering, and one have, to the leading order,

$$\delta H^{(1)}_{+i} \simeq \frac{e}{T_i} F_0 \left(1 - \frac{\omega_{*i}}{\omega}\right)_+ J_+ \delta\phi_+, \tag{69}$$

$$\delta H^{(1)}_{+e} \simeq -\frac{e}{T_e} F_0 \left(1 - \frac{\omega_{*e}}{\omega}\right)_+ \delta\psi_+. \tag{70}$$

The nonlinear ion response to Ω_+ can be derived as

$$\delta H^{(2)}_{+,i} \simeq -i \frac{\Lambda^s_0}{2\omega_0} J_0 J_s \frac{e}{T_i} F_0 \left(\frac{\omega_{*i}}{\omega}\right)_s \delta\phi_s \delta\phi_0, \tag{71}$$

with the linear ion response to Ω_0 and Ω_s noted. On the other hand, nonlinear electron contribution to upper KAW can be neglected as Ω_s is predominantly electrostatic. Substituting the particle responses into quasi-neutrality condition, we then have,

$$\delta\psi_+ = \sigma_{*+}\delta\phi_+ + i\frac{\Lambda_0^s}{2\omega_0}D_+\delta\phi_0\delta\phi_s, \tag{72}$$

where $\sigma_{*k} = [1 + \tau - \tau\Gamma_k(1 - \omega_{*i}/\omega)_k]/(1 - \omega_{*e}/\omega)_k$ denotes the deviation from ideal MHD condition due to plasma nonuniformity and/or FLR effects, while $D_+ = \tau(\omega_{*i}/\omega)_s F_+/(1 - \omega_{*e}/\omega)_+$ denotes nonlinear contribution with $F_+ = \langle J_0 J_s J_+ F_{M0}/N_0\rangle_v$. The other equation for Ω_+, can be derived from nonlinear vorticity equation, by substituting linear particle responses to Ω_0 and Ω_s into Reynolds stress term

$$\begin{aligned}&\tau b_+\left[\left(1-\frac{\omega_{*i}}{\omega}\right)_+\frac{(1-\Gamma_+)}{b_+}\delta\phi_+ - \left(\frac{V_A^2}{b}\frac{k_\parallel b k_\parallel}{\omega^2}\right)_+\delta\psi_+\right]\\ &= -i\frac{\Lambda_0^s}{2\omega_0}\gamma_+\delta\phi_0\delta\phi_s,\end{aligned} \tag{73}$$

with $\gamma_+ = \tau[\Gamma_s - \Gamma_0 + (\omega_{*i}/\omega)_s(F_+ - \Gamma_s)]$.

Combining equations (72) and (73), one obtains, the equation for upper KAW generation due to Ω_0 and Ω_s coupling

$$\tau b_+\epsilon_{A+}\delta\phi_+ = -i(\Lambda_0^s/2\omega_0)\beta_+\delta\phi_s\delta\phi_0, \tag{74}$$

where ϵ_{A+} is the linear SAW/KAW operator given by equation (16) with curvature coupling term neglected due to the interested TAE frequency range, and

$$\beta_+ = \tau(\Gamma_s - \Gamma_0) + \tau\left(\frac{\omega_{*i}}{\omega}\right)_s\left[F_+ - \Gamma_s - \left(\frac{k_\parallel b k_\parallel}{\omega^2}\right)_+\frac{\tau V_A^2 F_+}{(1-\omega_{*e}/\omega)_+}\right]. \tag{75}$$

The generation of lower KAW Ω_- due to Ω_0^* and Ω_s coupling, can be derived similarly as

$$\tau b_-\epsilon_{A-}\delta\phi_- = i(\Lambda_0^s/2\omega_-)\beta_-\delta\phi_s\delta\phi_0^*, \tag{76}$$

with

$$\beta_- = \tau(\Gamma_s - \Gamma_0) + \tau\left(\frac{\omega_{*i}}{\omega}\right)_s\left[F_- - \Gamma_s - \left(\frac{k_\parallel b k_\parallel}{\omega^2}\right)_-\frac{\tau V_A^2 F_-}{(1-\omega_{*e}/\omega)_-}\right]. \tag{77}$$

3.3.2 Feedback to Ω_0 and consequence on TAE stability

The effect of eDW scattering on the test TAE stability, can be derived by accounting for feedback of $\Omega_\pm$ via nonlinear coupling to Ω_s. Here, we give the nonlinear contribution to Ω_0 by nonlinear coupling between Ω_+ and Ω_s^*, while the contribution due to Ω_- and Ω_s coupling can be derived similarly, and we will only reinstate the effects in equation (85).

The nonlinear ion response to Ω_0 can be derived as

$$\delta H^{(2)}_{0i} \simeq \frac{e}{T_i} F_{0i}\left(\frac{\omega_{*i}}{\omega}\right)_s \left[i\frac{\Lambda^s_0}{2\omega_0} J_s J_+ \delta\phi^*_s \delta\phi_+ + \left(\frac{\Lambda^s_0}{2\omega_0}\right)^2 J_0 J^2_s |\delta\phi_s|^2 \delta\phi_0 \right] + \delta\phi_- \text{ contribution}, \tag{78}$$

with the second term from $\delta H^{(2)}_{+i}$ contribution. The nonlinear electron response to Ω_0 is negligible. The quasi-neutrality condition then yields

$$\delta\psi_0 = \left(\sigma_{*0} + \alpha_0 |\delta\phi_s|^2\right)\delta\phi_0 - i(\Lambda^s_0/2\omega_0) D^+_0 \delta\phi^*_s \delta\phi_+ + \delta\phi_- \text{ contribution}, \tag{79}$$

with $\alpha_0 = -(\Lambda^s_0/2\omega_0)^2 \tau(\omega_{*i}/\omega)_s F_2$, $F_2 \equiv \langle J^2_0 J^2_s F_{Mi}/N_0\rangle_v$ mainly contributing to nonlinear frequency shift, while $D^+_0 = \tau(\omega_{*i}/\omega)_s F_+/(1-\omega_{*e}/\omega)_0$.

The other equation for Ω_0 can then be derived from nonlinear vorticity equation, as

$$\tau b_0 \left\{ \left[\left(1 - \frac{\omega_{*i}}{\omega_0}\right)_0 \frac{(1-\Gamma_0)}{b_0} + \alpha^+_0 |\delta\phi_s|^2 \right] \delta\phi_0 - \left(\frac{V^2_A}{b}\frac{k_\parallel b k_\parallel}{\omega^2}\right)_0 \delta\psi_0 \right\} = i\frac{\Lambda^s_0}{2\omega_0}\gamma^+_0 \delta\psi^*_s \delta\phi_+ + \delta\phi_- \text{ contribution}. \tag{80}$$

Substituting equation (79) into (80), and neglecting the nonlinear frequency shift while focusing on the stability of the test TAE due to scattering by background eDW, one then obtains

$$\tau b_0 \epsilon_{A0} \delta\phi_0 = i\frac{\Lambda^s_0}{2\omega_0}\beta^+_0 \delta\phi^*_s \delta\phi_+ + \delta\phi_- \text{ contribution}. \tag{81}$$

Substituting $\delta\phi_+$ from equation (74) into (81), one obtains,

$$\tau b_0 \epsilon_{A0} \delta\phi_0 = \left[\left(\frac{\Lambda^s_0}{2\omega_0}\right)^2 \beta^+_0 \delta\phi^*_s \frac{\beta_+}{\tau b_+ \epsilon_{A+}} \delta\phi_s \right] \delta\phi_0 + \delta\phi_- \text{ contribution}, \tag{82}$$

which can be solved noting the scale separation between $\delta\phi_0$ and $\delta\phi_s$, as sketched in Fig. 8. Thus, the nonlinear coupling processes occur in in a narrow region of the eDW localization. Expanding $\delta\phi_0 = \Phi_0(\mathbf{x}_0) + \tilde{\Phi}_0(\mathbf{x}_s, \mathbf{x}_0)$ with $\mathbf{x}_0 = (R/n_0, r/m_0, 1/n_0 q')$, $\mathbf{x}_s = (R/n_s, r/m_s, 1/n_s q')$ and $|\tilde{\Phi}_0|/|\Phi_0| \sim O(|e\delta\phi_s/T_e|^2) \ll 1$, equation (82) becomes, after averaging over $\mathbf{x}_s$ scale,

$$\tau b_0 \epsilon_{A0} \Phi_0 = \left\langle \left(\frac{\Lambda^s_0}{2\omega_0}\right)^2 \beta^+_0 \delta\phi^*_s \frac{\beta_+}{\tau b_+ \epsilon_{A+}} \delta\phi_s \right\rangle_s \Phi_0 + \delta\phi_- \text{ contribution}, \tag{83}$$

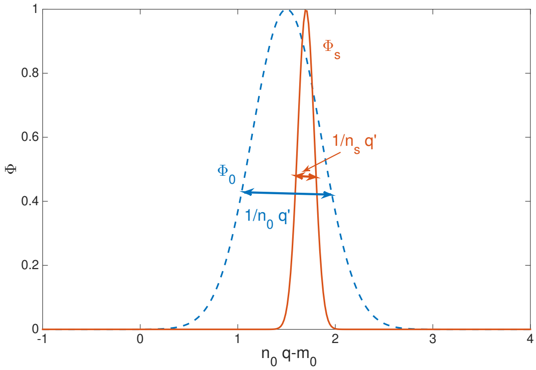

Fig. 8 Cartoon of scale separation between TAE and eDW, with the dashed curve being the sketched parallel mode structure of a TAE poloidal harmonic, while the solid curve being the parallel mode structure of eDW with much smaller radial width than that of the TAE.

with $\langle\cdots\rangle_s$ denoting averaging over eDW scales

$$\langle(\cdots)|\delta\phi_s|_s\rangle_s \equiv |A_{n_s}|^2 \int_{\infty}^{\infty} dz_s(\cdots)|\Phi_s(z_s)|^2. \tag{84}$$

Equation (83) can then be solved noting that the stability induced by $\mathrm{Im}(1/\epsilon_{A+})$ can be expressed as $\mathrm{Im}(1/\epsilon_{A+}) = -\pi\delta(\epsilon_{A+}) \simeq -(\pi/4\sigma_{*+})\delta(z_s^2 - z_+^2)$ with $z_+^2 = (1-\omega_{*i}/\omega)_+(1-\Gamma_+)(\omega/\omega_A)_+^2/(b_+\sigma_{*+})$, which implies KAW being absorbed locally, expanding β_+ with respect to b_s noting two scale separation $k_{+\perp}^2 \simeq k_{s\perp}^2 + 2k_{sr}k_{0r}$, and properly reinstating the lower KAW contribution, one then obtains,

$$\tau b_0\left[\epsilon_{A0} + i\nu(k_{0r}\rho_i)^2\right]\Phi_0 = 0, \tag{85}$$

with $\nu = \nu_+ + \nu_-$, and

$$\nu_\pm \simeq \pi\left(\frac{\Omega_{ci}}{\omega_0}\right)^2 \sum_{n_s}|A_{n_s}|^2\left[\left(\tau + \frac{\sigma_s}{2\Gamma_s}\right)\frac{\partial\Gamma_s}{\partial b_{s\theta}}\right]^2 \frac{b_{s\theta}\hat{s}^2}{\sigma_{s\pm}^2 z_\pm}\left|\frac{\partial\Phi_s}{\partial z_s}\right|_{z_\pm}^2. \tag{86}$$

Equation (85) can be solved perturbatively in ballooning space, η. I.e., letting $\hat{\Phi}_0(\eta)$ being the lowest order eigenmode satisfying $\hat{b}_0\hat{\epsilon}_{A0}(\eta,\partial_\eta,\omega_0)\hat{\Phi}_0(\eta)$, and expanding $\omega_0 = \omega_{0r} + i\gamma_{AD}$ with γ_{AD} being the eDW scattering induced test TAE damping rate, equation (85) then gives,

$$\frac{2\gamma_{AD}}{\omega_{0r}}\left\langle\hat{\Phi}_0\hat{b}_0\hat{\Phi}_0\right\rangle_\eta = -\left\langle\hat{\Phi}_0\hat{b}_0\nu b_{0\theta}\hat{s}^2\eta^2\hat{\Phi}_0\right\rangle, \tag{87}$$

with $\langle\cdots\rangle_\eta \equiv \int_{-\infty}^{\infty}(\cdots)d\eta$. Noting equation (24) for TAE, we obtain

$$\frac{\gamma_{AD}}{\omega_{0r}} = -\frac{1}{4}\frac{\nu b_{0\theta}\hat{s}^2}{\sqrt{-\Gamma_l\Gamma_u}} \sim O(10^{-2}-10^{-1}), \tag{88}$$

as estimated using typical parameters, i.e., $|\Omega_{ci}/\omega_{0r}| \sim O(10^2)$, $\sum_{n_s}|A_{n_s}|^2 \sim |e\delta\phi_s/T_e|^2 \sim O(10^{-4})$, $b_{s\theta} \sim \hat{s} \sim \tau \sim O(1)$ and $4\sqrt{-\Gamma_l\Gamma_u} \sim O(\epsilon^2) \sim O(10^{-2}-10^{-1})$. The eDW scattering induced TAE damping rate is comparable to the TAE growth rate due to EP drive [5], and can significantly reduce or completely suppress TAE fluctuations with sufficiently large eDW intensity. This may imply improved fusion alpha particle confinement in the existence of micro turbulence, and consequently, enhanced thermal plasma heating.

As the nonlinearly generated KAW quasi-modes are dissipated by predominantly electron Landau damping [8, 9], the resulting electron heating rate can be estimated as

$$\left(\frac{d\beta_e}{dt}\right)_{AD} = 4|\gamma_{AD}|\left|\frac{\delta B_\perp}{B_0}\right|^2 \simeq O(10^{-2}-10^{-1})s^{-1}, \tag{89}$$

which, for typical parameters, can be comparable to the electron heating by alpha particle slowing down, and potentially, contribute significantly to the "anomalous" electron heating in burning plasmas.

The present analysis, using TAE scattering by ambient eDW as an example to demonstrate the novel physics of direct cross-scale interaction among meso/macro-scale SAW instabilities and micro-scale DW turbulence, and the obtained results are expected to be, at least, qualitatively applicable to other Alfvén eigenmodes such as reversed shear Alfvén eigenmode (RSAE), and include the physics of finite temperature gradients or trapped electrons. These application to more realistic scenarios can be investigated for a more thorough understanding of the SAW stabilities and thus fusion alpha particle confinement in reactors.

4 Summary

Using toroidal Alfvén eigenmode (TAE) nonlinear saturation due to mode-mode coupling as example, we show that, nonlinear gyrokinetic theory is not only powerful, but also necessary to investigate various crucial physics in the nonlinear mode coupling processes of SAW instabilities. This necessity occurs since SAW instabilities often have a small scale structure associated with the SAW continuum related to equilibrium magnetic geometry and plasma nonuniformity of magnetically confined fusion devices. The nonlinear coupling is, thus, dominated through perpendicular scattering [33]. Three main processes developed in the past decade are briefly reviewed, i.e., the zonal field structure (ZFS) generation by TAE [39], TAE spectral cascading due to ion induced scattering [35, 36], and cross-scale interaction with electron drift wave (eDW) via direct nonlinear interaction [47]. The fundamental physics involved in the three processes are reviewed in a pedagogical way, with parameter regimes for them to occur and dominate discussed, and state-of-art developments as well as open questions are also introduced. These understandings present a road map for a comprehensive and quantitative study of SAW instability spectrum in reactors, and provide guidance for large scale simulations using realistic geometry and plasma parameters.

It is obvious that, the nonlinear mode coupling process reviewed in the present work, and the self-consistent EP transport, should be considered on the same footing for the comprehensive understanding of the SAW instability nonlinear dynamics and self-consistent EP transport. The former, described by the nonlinear radial envelope equation in the form of a nonlinear Schr*ö*dinger equation, together with the latter described by the Dyson-Schr*ö*dinger model, constitute a general theoretical framework for SAW nonlinear dynamics and EP transport in burning plasma physics [5, 24, 25], and is the ongoing effort of Center for Nonlinear Plasma Science (CNPS) collaboration.

Acknowledgement

This work was supported by the National Science Foundation of China under Grant Nos. 12275236 and 12261131622, and "Users of Excellence program of Hefei Science Center CAS" under Contract No. 2021HSC-UE016. This work was was supported by the EUROfusion Consortium, funded by the European Union via the Euratom Research and Training Programme (Grant Agreement No. 101052200 EUROfusion). The views and opinions expressed are, however, those of the author(s) only and do not necessarily reflect those of the European Union or the European Commission. Neither the European Union nor the European Commission can be held responsible for them.

References

[1] Alfvén, H.: Existence of electromagnetic-hydrodynamic waves. Nature **150**(3805), 405–406 (1942)

[2] Tomabechi, K., Gilleland, J.R., Sokolov, Y.A., Toschi, R., Team, I.: Iter conceptual design. Nuclear Fusion **31**(6), 1135 (1991)

[3] Wan, Y., Li, J., Liu, Y., Wang, X., Chan, V., Chen, C., Duan, X., Fu, P., Gao, X., Feng, K., *et al.*: Overview of the present progress and activities on the cfetr. Nuclear Fusion **57**(10), 102009 (2017)

[4] Fasoli, A., Gormenzano, C., Berk, H.L., Breizman, B., Briguglio, S., Darrow, D.S., Gorelenkov, N., Heidbrink, W.W., Jaun, A., Konovalov, S.V., Nazikian, R., Noterdaeme, J.-M., Sharapov, S., Shinohara, K., Testa, D., Tobita, K., Todo, Y., Vlad, G., Zonca, F.: Chapter 5: Physics of energetic ions. Nuclear Fusion **47**(6), 264 (2007)

[5] Chen, L., Zonca, F.: Alfvén waves and energetic particles. Review of Modern Physics **88**(1), 015008 (2016)

[6] Grad, H.: Plasmas. Physics Today **22**(12), 34 (1969)

[7] Chen, L., Hasegawa, A.: Plasma heating by spatial resonance of alfven wave. The Physics of Fluids **17**(7), 1399–1403 (1974)

[8] Hasegawa, A., Chen, L.: Kinetic processes in plasma heating by resonant mode conversion of alfvén wave. Physics of Fluids **19**(12), 1924–1934 (1976)

[9] Chen, L., Zonca, F., Lin, Y.: Physics of kinetic alfvén waves: a gyrokinetic theory approach. Reviews of Modern Plasma Physics **5**(1), 1–37 (2021)

[10] Chen, L.: Theory of magnetohydrodynamic instabilities excited by energetic particles in tokamaks. Physics of Plasmas **1**(5), 1519 (1994)

[11] Cheng, C.Z., Chen, L., Chance, M.S.: High-n ideal and resistive shear alfvén waves in tokamaks. Ann. Phys. **161**, 21 (1985)

[12] Chen, L.: On resonant excitation of high-n magnetohydrodynamic modes by energetic/alpha particles in tokamaks. In: Vaclavik, J., Troyon, F., Sindoni, E. (eds.) Theory of Fusion Plasmas, p. 327. Association EUROATOM, Bologna, ??? (1988)

[13] Fu, G.Y., Van Dam, J.W.: Excitation of the toroidicity induced shear alfvén eigenmode by fusion alpha particles in an ignited tokamak. Physics of Fluids B **1**(10), 1949–1952 (1989)

[14] Wong, K.L., Fonck, R.J., Paul, S.F., Roberts, D.R., Fredrickson, E.D., Nazikian, R., Park, H.K., Bell, M., Bretz, N.L., Budny, R., Cohen, S., Hammett, G.W., Jobes, F.C., Meade, D.M., Medley, S.S., Mueller, D., Nagayama, Y., Owens, D.K., Synakowski, E.J.: Excitation of toroidal alfvén eigenmodes in tftr. Phys. Rev. Lett. **66**, 1874–1877 (1991)

[15] Vlad, G., Zonca, F., Briguglio, S.: Dynamics of alfvén waves in tokamaks. La Rivista del Nuovo Cimento (1978-1999) **22**(7), 1 (1999)

[16] Zonca, F., Chen, L.: Theory on excitations of drift alfvén waves by energetic particles. ii. the general fishbone-like dispersion relation. Physics of Plasmas **21**(7), 072121 (2014)

[17] Todo, Y.: Introduction to the interaction between energetic particles and alfven eigenmodes in toroidal plasmas. Reviews of Modern Plasma Physics **3**(1) (2019)

[18] Chen, L.: Theory of plasma transport induced by low-frequency

hydromagnetic waves. Journal of Geophysical Research: Space Physics **104**(A2), 2421 (1999)

[19] Chen, L., Hasegawa, A.: Kinetic theory of geomagnetic pulsations: 1. internal excitations by energetic particles. Journal of Geophysical Research: Space Physics **96**(A2), 1503 (1991)

[20] Berk, H.L., Breizman, B.N.: Saturation of a single mode driven by an energetic injected beam. i. plasma wave problem. Physics of Fluids B **2**(9), 2226 (1990)

[21] Berk, H.L., Breizman, B.N.: Saturation of a single mode driven by an energetic injected beam. ii. electrostatic universal destabilization mechanism. Physics of Fluids B **2**(9), 2235 (1990)

[22] Berk, H.L., Breizman, B.N.: Saturation of a single mode driven by an energetic injected beam. iii. alfvén wave problem. Physics of Fluids B **2**(9), 2246 (1990)

[23] O'Neil, T.: Collisionless damping of nonlinear plasma oscillations. Physics of Fluids **8**(12), 2255–2262 (1965)

[24] Zonca, F., Chen, L., Falessi, M., Qiu, Z.: Nonlinear radial envelope evolution equations and energetic particle transport in tokamak plasmas. Journal of Physics: Conference Series **1785**(1), 012005 (2021)

[25] Zonca, F., Chen, L., Briguglio, S., Fogaccia, G., Vlad, G., Wang, X.: Nonlinear dynamics of phase space zonal structures and energetic particle physics in fusion plasmas. New Journal of Physics **17**(1), 013052 (2015)

[26] Falessi, M.V., Zonca, F.: Transport theory of phase space zonal structures. Physics of Plasmas **26**(2), 022305 (2019)

[27] Falessi, M., Chen, L., Qiu, Z., Zonca, F. to be submitted to New Journal of Physics (2022)

[28] Wang, X., Briguglio, S., Chen, L., Di Troia, C., Fogaccia, G., Vlad, G., Zonca, F.: Nonlinear dynamics of beta-induced alfvén eigenmode driven by energetic particles. Phys. Rev. E **86**, 045401 (2012)

[29] Zhang, H.S., Lin, Z., Holod, I.: Nonlinear frequency oscillation of alfvén eigenmodes in fusion plasmas. Phys. Rev. Lett. **109**, 025001 (2012)

[30] Yu, L., Zonca, F., Qiu, Z., Chen, L., Chen, W., Ding, X., Ji, X., Wang, T., Wang, T., Ma, R., *et al.*: Experimental evidence of nonlinear avalanche dynamics of energetic particle modes. Europhysics Letters **138**(5), 54002 (2022)

[31] Wang, T., Qiu, Z., Zonca, F., Briguglio, S., Fogaccia, G., Vlad, G., Wang, X.: Shear alfvén fluctuation spectrum in divertor tokamak test facility plasmas. Physics of Plasmas **25**(6), 062509 (2018)

[32] Ren, Z., Chen, Y., Fu, G., Wang, Z.: Stability of alfvén eigenmodes in the china fusion engineering test reactor. Nuclear Fusion **60**(1), 016009 (2020)

[33] Chen, L., Zonca, F.: Gyrokinetic theory of parametric decays of kinetic alfvén waves. Europhysics Letters **96**(3), 35001 (2011)

[34] Sagdeev, R., Galeev., A.: Nonlinear Plasma Theory. AW Benjamin Inc., ??? (1969)

[35] Hahm, T.S., Chen, L.: Nonlinear saturation of toroidal alfvén eigenmodes via ion compton scattering. Phys. Rev. Lett. **74**, 266 (1995)

[36] Qiu, Z., Chen, L., Zonca, F.: Gyrokinetic theory of the nonlinear saturation of a toroidal alfvén eigenmode. Nuclear Fusion **59**(6), 066024 (2019)

[37] Rosenbluth, M.N., Hinton, F.L.: Poloidal flow driven by ion-temperature-gradient turbulence in tokamaks. Phys. Rev. Lett. **80**, 724–727 (1998)

[38] Chen, L., Lin, Z., White, R.: Excitation of zonal flow by drift waves in toroidal plasmas. Physics of Plasmas **7**(8), 3129–3132 (2000)

[39] Chen, L., Zonca, F.: Nonlinear excitations of zonal structures by toroidal alfvén eigenmodes. Phys. Rev. Lett. **109**, 145002 (2012)

[40] Frieman, E.A., Chen, L.: Nonlinear gyrokinetic equations for low-frequency electromagnetic waves in general plasma equilibria. Physics of Fluids **25**(3), 502–508 (1982)

[41] Chen, L., Zonca, F.: On nonlinear physics of shear alfvén waves. Physics of Plasmas **20**(5), 055402 (2013)

[42] Kieras, C., Tataronis, J.: The shear alfvén continuous spectrum of axisymmetric toroidal equilibria in the large aspect ratio limit. Journal of Plasma Physics **28**(3), 395 (1982)

[43] Brizard, A.J., Hahm, T.S.: Foundations of nonlinear gyrokinetic theory. Rev. Mod. Phys. **79**, 421 (2007)

[44] Todo, Y., Berk, H., Breizman, B.: Nonlinear magnetohydrodynamic effects on alfvén eigenmode evolution and zonal flow generation. Nuclear Fusion **50**(8), 084016 (2010)

[45] Qiu, Z., Chen, L., Zonca, F.: Effects of energetic particles on zonal flow generation by toroidal alfvén eigenmode. Physics of Plasmas (1994-present) **23**(9), 090702 (2016)

[46] Chen, L., Lin, Z., White, R.B., Zonca, F.: Nonlinear zonal dynamics of drift and drift-alfvén turbulence in tokamak plasmas. Nuclear fusion **41**(6), 747 (2001)

[47] Chen, L., Qiu, Z., Zonca, F.: On scattering and damping of toroidal alfvén eigenmode by drift wave turbulence. Nuclear Fusion **62**(9), 094001 (2022)

[48] Citrin, J., Jenko, F., Mantica, P., Told, D., Bourdelle, C., Garcia, J., Haverkort, J., Hogeweij, G., Johnson, T., Pueschel, M.: Nonlinear stabilization of tokamak microturbulence by fast ions. Physical review letters **111**(15), 155001 (2013)

[49] Di Siena, A., Görler, T., Poli, E., Navarro, A.B., Biancalani, A., Jenko, F.: Electromagnetic turbulence suppression by energetic particle driven modes. Nuclear Fusion **59**(12), 124001 (2019)

[50] Mazzi, S., Garcia, J., Zarzoso, D., Kazakov, Y.O., Ongena, J., Dreval, M., Nocente, M., Štancar, Ž., Szepesi, G., Eriksson, J., *et al.*: Enhanced performance in fusion plasmas through turbulence suppression by mega-electronvolt ions. Nature Physics **18**(7), 776–782 (2022)

[51] Lin, Z., Hahm, T.S., Lee, W.W., Tang, W.M., White, R.B.: Turbulent transport reduction by zonal flows: Massively parallel simulations. Science **281**(5384), 1835–1837 (1998)

[52] Zonca, F., White, R.B., Chen, L.: Nonlinear paradigm for drift wave–zonal flow interplay: Coherence, chaos, and turbulence. Physics of Plasmas **11**(5), 2488–2496 (2004)

[53] Diamond, P.H., Itoh, S.-I., Itoh, K., Hahm, T.S.: Zonal flows in plasma: a review. Plasma Physics and Controlled Fusion **47**(5), 35 (2005)

[54] Spong, D., Carreras, B., Hedrick, C.: Nonlinear evolution of the toroidal alfvén instability using a gyrofluid model. Physics of plasmas **1**(5), 1503 (1994)

[55] Zonca, F., Lin, Y., Chen, L.: Spontaneous excitation of convective cells by kinetic alfvén waves. Europhysics Letters **112**(6), 65001 (2015)

[56] Qiu, Z., Chen, L., Zonca, F.: Nonlinear excitation of finite-radial-scale zonal structures by toroidal alfvén eigenmode. Nuclear Fusion **57**(05), 056017 (2017)

[57] Qiu, Z., Chen, L., Zonca, F.: Spontaneous excitation of geodesic acoustic mode by toroidal alfvén eigenmodes. Europhysics Letters **101**(3), 35001 (2013)

[58] Qiu, Z., Chen, L., Zonca, F.: Fine radial structure zonal flow excitation by beta-induced alfvén eigenmode. Nuclear Fusion **56**(10), 106013 (2016)

[59] Zhang, H., Lin, Z.: Nonlinear generation of zonal fields by the beta-induced alfvén eigenmode in tokamak. Plasma Science and Technology **15**(10), 969 (2013)

[60] Wei, S., Wang, T., Chen, N., Qiu, Z.: Nonlinear reversed shear alfvén eigenmode saturation due to spontaneous zonal current generation. Journal of Plasma Physics **87**(5), 905870505 (2021)

[61] Heidbrink, W.W., Gorelenkov, N.N., Luo, Y., Van Zeeland, M.A., White, R.B., Austin, M.E., Burrell, K.H., Kramer, G.J., Makowski, M.A., McKee, G.R., Nazikian, R.: Anomalous flattening of the fast-ion profile during alfvén-eigenmode activity. Phys. Rev. Lett. **99**, 245002 (2007)

[62] Biancalani, A., Bottino, A., Siena, A.D., Gurcan, O., Hayward-Schneider, T., Jenko, F., Lauber, P., Mishchenko, A., Morel, P., Novikau, I., Vannini, F., Villard, L., Zocco, A.: Gyrokinetic investigation of alfvén instabilities in the presence of turbulence. Plasma Physics and Controlled Fusion **63**(6), 065009 (2021)

[63] Hahm, T.S.: Ion heating from nonlinear landau damping of high mode number toroidal alfvén eigenmodes. Plasma Science and Technology **17**(7), 534 (2015)

[64] Fisch, N.J., Herrmann, M.C.: Utility of extracting alpha particle energy by waves. Nuclear Fusion **34**(12), 1541 (1994)

[65] Fisch, N.J., Rax, J.-M.: Interaction of energetic alpha particles with intense lower hybrid waves. Phys. Rev. Lett. **69**, 612–615 (1992)

[66] Qiu, Z., Chen, L., Zonca, F., Chen, W.: Nonlinear decay and plasma heating by a toroidal alfvén eigenmode. Phys. Rev. Lett. **120**(13), 135001 (2018)

[67] Qiu, Z., Chen, L., Zonca, F., Chen, W.: Nonlinear excitation of a geodesic acoustic mode by toroidal alfvén eigenmodes and the impact on plasma performance. Nuclear Fusion **59**(6), 066031 (2019)

[68] Wei, S., Wang, T., Chen, L., Zonca, F., Qiu, Z.: Core localized alpha-channeling via low frequency alfvén mode generation in reversed shear scenarios. Nuclear Fusion **62**(12), 126038 (2022)

[69] Wang, T., Wang, X., Briguglio, S., Qiu, Z., Vlad, G., Zonca, F.: Nonlinear dynamics of shear alfvén fluctuations in divertor tokamak test facility plasmas. Physics of Plasmas **26**(1), 012504 (2019)

[70] Brizard, A.J.: Nonlinear gyrokinetic vlasov equation for toroidally rotating axisymmetric tokamaks. Physics of Plasmas **2**(2), 459–471 (1995)

[71] Fu, G., Cheng, C.: Excitation of high-n toroidicity-induced shear alfvén eigenmodes by energetic particles and fusion allpha-particles in tokamaks. Physics of Fluids B - Plasma Physics **4**(11), 3722 (1992)

[72] Chen, L., Qiu, Z., Zonca, F.: Parity-breaking parametric decay instability of kinetic alfvén waves in a nonuniform plasma. Physics of Plasmas **29**(5), 050701 (2022)

[73] Cheng, Z., Shen, K., Chen, L., Zonca, F., Qiu, Z.: Effects of plasma non-uniformity on toroidal Alfvén eigenmode nonlinear saturation via ion induced scattering (2023)

[74] Chen, L., Qiu, Z., Zonca, F.: On Nonlinear Scattering of Drift Wave by Toroidal Alfvén Eigenmode in Tokamak Plasmas (2023)

[75] Horton, W.: Drift waves and transport. Rev. Mod. Phys. **71**, 735–778 (1999)

[76] Zhang, W., Lin, Z., Chen, L.: Transport of energetic particles by microturbulence in magnetized plasmas. Phys. Rev. Lett. **101**(9), 095001 (2008)

[77] Feng, Z., Qiu, Z., Sheng, Z.: The mechanism of particles transport induced by electrostatic perturbation in tokamak. Physics of Plasmas **20**(12), (2013)

[78] Tardini, G., Hobirk, J., Igochine, V., Maggi, C., Martin, P., McCune, D., Peeters, A., Sips, A., Stäbler, A., Stober, J., *et al.*: Thermal ions dilution and itg suppression in asdex upgrade ion itbs. Nuclear fusion **47**(4), 280 (2007)

[79] Bourdelle, C., Hoang, G., Litaudon, X., Roach, C., Tala, T.: Impact of the α parameter on the microstability of internal transport barriers. Nuclear fusion **45**(2), 110 (2005)

[80] Citrin, J., Mantica, P.: Overview of tokamak turbulence stabilization by fast ions. Plasma Physics and Controlled Fusion **65**(3), 033001 (2023)

[81] Di Siena, A., Gorler, T., Poli, E., Banon Navarro, A., Biancalani, A., Bilato, R., Bonanomi, N., Novikau, I., Vannini, F., Jenko, F.: Nonlinear

electromagnetic interplay between fast ions and ion-temperature-gradient plasma turbulence. Journal of Plasma Physics **87**(2), 555870201 (2021)